The Journal of Neuroscience, August 1, 1996, *16*(15):4757–4775

Divergent Projections from the Anterior Inferotemporal Area TE to the Perirhinal and Entorhinal Cortices in the Macaque Monkey

K. S. Saleem[1] **and K. Tanaka**[1,2]

[1]*Laboratory for Neural Information Processing, Frontier Research Program, and* [2]*Information Science Laboratory, Institute of Physical and Chemical Research (RIKEN), Wako-shi, Saitama 351-01, Japan*

Area TE is located at the latter part of the ventral visual cortical pathway, which is essential for visual recognition of objects. TE projects heavily to the perirhinal region, which is important for visual recognition memory of objects. To study the organization of projections from TE to the perirhinal (areas 35 and 36) and entorhinal (area 28) cortices, we made focal injections of *Phaseolus vulgaris* leucoagglutinin (PHA-L) and large injections of biocytin or wheat germ agglutinin conjugated to horseradish peroxidase (WGA-HRP) into anterior levels of TE in macaque monkeys. Injections of PHA-L into the ventral part of anterior TE (TEav) resulted in labeling of terminals distributed widely in area 36 (approximately one-half of its total extent), although the injection sites were limited to 0.7 mm in width. The labeled terminals tended to be denser in the medial part of area 36. There was less dense but definite labeling in area 35 and the lateral part of area 28. After a single injection of PHA-L or WGA-HRP into the dorsal part of anterior TE (TEad), labeled terminals were confined to a small region at the lateral part of area 36 (less than one-tenth of its total extent). The projections to areas 35 and 28 from TEad were much sparser than those from TEav.

The different patterns of projections to the perirhinal and entorhinal cortices, together with previously reported differences in their afferent and other efferent connections, suggest the functional differentiation between TEav and TEad. The divergent projection from TEav to the perirhinal cortex may facilitate the association of different visual features in the perirhinal cortex.

Key words: inferotemporal cortex; area TE; perirhinal cortex; entorhinal cortex; PHA-L; single axon; laminar organization; macaque monkey

Area TE of the inferotemporal cortex of the macaque monkey is an extrastriate visual cortical area, located at the latter part of the ventral visual pathway. TE is thought to be important for object vision, that is, the discrimination and recognition of visual images of objects. Monkeys with bilateral TE lesions show severe and specific deficits in learning tasks that require these functions (for review, see Gross, 1973; Dean, 1976). Cells in TE respond selectively to particular features of complex objects (for review, see Tanaka, 1996), and cells with similar selectivities are clustered in local columnar regions in TE (Fujita et al., 1992). TE projects to several polymodal brain sites including the perirhinal cortex, the frontal cortex, the amygdala, and the striatum. The cortical connection from TE to the perirhinal cortex is the subject of the present study.

The perirhinal cortex (areas 35 and 36) is a medial temporal lobe structure, located on the ventromedial aspect of the anterior temporal cortex. Recent behavioral studies showed that combined lesions of the perirhinal and entorhinal cortices (Gaffan and Murray, 1992; Murray, 1992; Meunier et al., 1993) and combined lesions of the perirhinal and parahippocampal cortices in the macaque monkey (Zola-Morgan et al., 1989; Suzuki et al., 1993) produced significant deficits in learning of tasks that required visual recognition memory of objects (delayed-matching- or nonmatching-to-sample task). There is also behavioral evidence that the perirhinal cortex is the most important for performance of the visual recognition memory task (Murray et al., 1993; Eacott et al., 1994; Gaffan, 1994; Leonard et al., 1995). The perirhinal cortex projects to the hippocampus via the entorhinal cortex (area 28) (Van Hoesen and Pandya, 1975b; Insausti et al., 1987; Witter and Amaral, 1991; Suzuki and Amaral, 1994a).

Although the global properties of the projection from TE to the perirhinal cortex have been studied previously in the macaque monkey using degeneration and anterograde tracer methods (Van Hoesen and Pandya, 1975a; Turner et al., 1980; Webster et al., 1991; Suzuki and Amaral, 1994b), little is known about the detailed organization of projection from TE to the perirhinal cortex. In particular, the pattern of divergence from a single site within TE, the detailed laminar distribution of the terminals, and differences in the projection from the dorsal and ventral parts of TE have not been investigated. To observe the divergence and the laminar pattern of terminations, injection of *Phaseolus vulgaris* leucoagglutinin (PHA-L) at a single site was used as the central technique in the present study. Differences in the projection from the different parts of TE were of particular interest because of the following recent anatomical and behavioral findings. Yukie et al. (1990) found that the anteroventral part of the cortex medial to the anterior middle temporal sulcus (TEav) and the anterodorsal part between the superior temporal sulcus and the anterior middle temporal sulcus (TEad) projected differentially to the amygdala and the hippocampus. Horel and his colleagues (Horel and Pytko, 1982; Horel et al., 1987) found that cooling limited to the anterior inferotemporal gyrus, including TEav and the perirhinal

Received Jan. 3, 1996; revised May 16, 1996; accepted May 17, 1996.

This work was supported by the Frontier Research Program, RIKEN, Japan. We thank Kathleen S. Rockland, Gary W. Van Hoesen, and David G. Amaral for helpful comments on this manuscript; K. Cheng and W. Suzuki for surgical assistance; and A. H. Asiya Begum for histological assistance.

Correspondence should be addressed to Kadharbatcha S. Saleem, Laboratory for Neural Information Processing, Frontier Research Program, RIKEN, 2-1 Hirosawa, Wako-shi, Saitama 351-01, Japan.

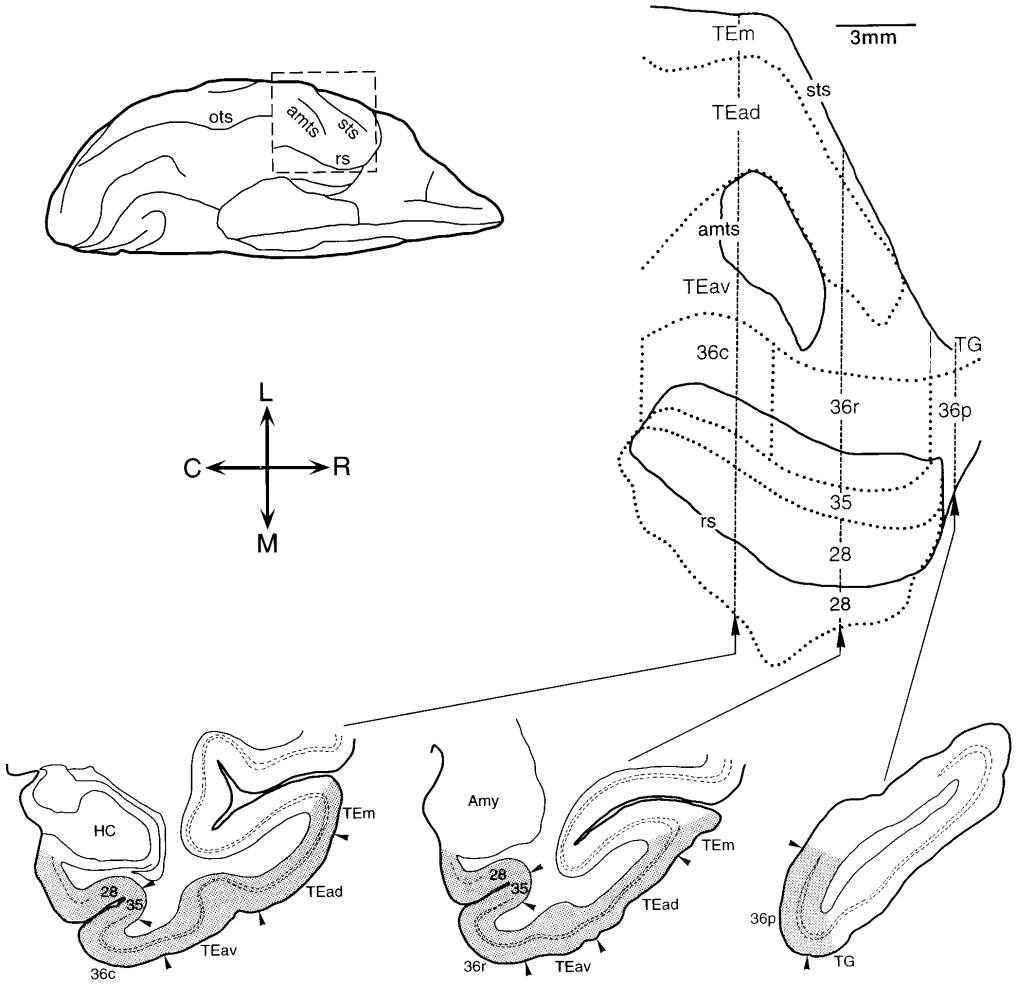

Figure 1. Location of the subdivisions of area TE, perirhinal cortex (areas 35 and 36), and the entorhinal cortex (area 28). A ventral view of the brain is shown at the *top left*. The portion of the brain circumscribed by the *broken line* was unfolded to produce the two-dimensional map shown at the *top right*. The *solid lines* indicate the lips of the sulci, and the *dotted lines* show the borders between cortical areas and their subdivisions. In contrast to the conventional unfolding, the coronal sections are represented by *vertical straight lines* in the map in this study. Camera lucida drawings of three representative coronal sections are shown at the *bottom*. *Shaded areas* in the coronal sections indicate the areas included in the two-dimensional map. *sts*, Superior temporal sulcus; *amts*, anterior middle temporal suclus; *rs*, rhinal sulcus; *ots*, occipitotemporal sulcus; *HC*, hippocampus; *Amy*, amygdala; *C*, caudal; *R*, rostral; *M*, medial; *L*, lateral.

cortex, produced deficits in performance of a delayed-matching-to-sample task, whereas cooling of TEad did not.

Some of the present results have been reported in abstract form (Saleem et al., 1993a, 1994).

MATERIALS AND METHODS

Ten Japanese monkeys (*Macaca fuscata*) of both sexes, weighing between 3.3 and 6.9 kg, were used. PHA-L was injected into the TEad in two monkeys and the TEav in two monkeys. Because we intended to observe the global pattern of projection from a single site, PHA-L was injected into a single site. The body weights of the monkeys in which PHA-L was injected ranged from 3.3 to 4.6 kg. Wheat germ agglutinin conjugated to horseradish peroxidase (WGA-HRP) was injected into TEav in one monkey and TEad in two monkeys to observe the projection patterns to the perirhinal and entorhinal cortices from large injection sites, as well as to see the distribution of neurons projecting back to TEav and TEad. WGA-HRP was injected into a single site except in one TEad case, in which nine injections were made to cover a larger part of TEad. In three monkeys, injection of WGA-HRP into TEad and biocytin into TEav were combined to compare the projection patterns from TEad and TEav in the same hemisphere. In each of these cases, WGA-HRP was injected into a single site and biocytin into two nearby sites (interval of <0.5 mm). Biocytin labeling failed in one case. Biocytin, but not PHA-L, was combined with WGA-HRP because we can use the same survival time for both biocytin and WGA-HRP. All of the injections were made in the right hemisphere except in one monkey, in which WGA-HRP was injected in the left hemisphere.

Surgery and injection. The tracers were injected during aseptic surgery under general anesthesia. After an initial treatment with atropine sulfate (0.1 mg/kg, i.m.), anesthesia was induced by intramuscular injection of ketamine hydrochloride (12 mg/kg), followed by intraperitoneal injection of sodium pentobarbital (Nembutal, 35 mg/kg). Supplemental doses of sodium pentobarbital (9 mg/kg, i.p.) were given as needed to maintain a surgical level of anesthesia. Tranexamic acid (25 mg/kg, i.m.) was given to minimize bleeding.

A large craniotomy was made over the ventrolateral temporal area after removing the zygomatic arch. The dura was resected to allow direct visualization of a large part of the superior temporal sulcus and the anterior middle temporal sulcus to determine the injection site. For TEav injections, 20 ml of 20% mannitol was injected into the monkey intravenously over 30–60 min to reduce the brain volume, so that the cortex medial to the anterior middle temporal sulcus became accessible. After the injection was completed, the dura was sutured and the wound was closed. Dexamethasone sodium phosphate (1 mg/kg, i.m.) was given to minimize the cerebral edema. The antibiotic piperacillin sodium (55 mg/kg, i.m.) and the analgesic ketoprofen (5 mg/kg, i.m.) were injected daily for 4–5 d after the surgery.

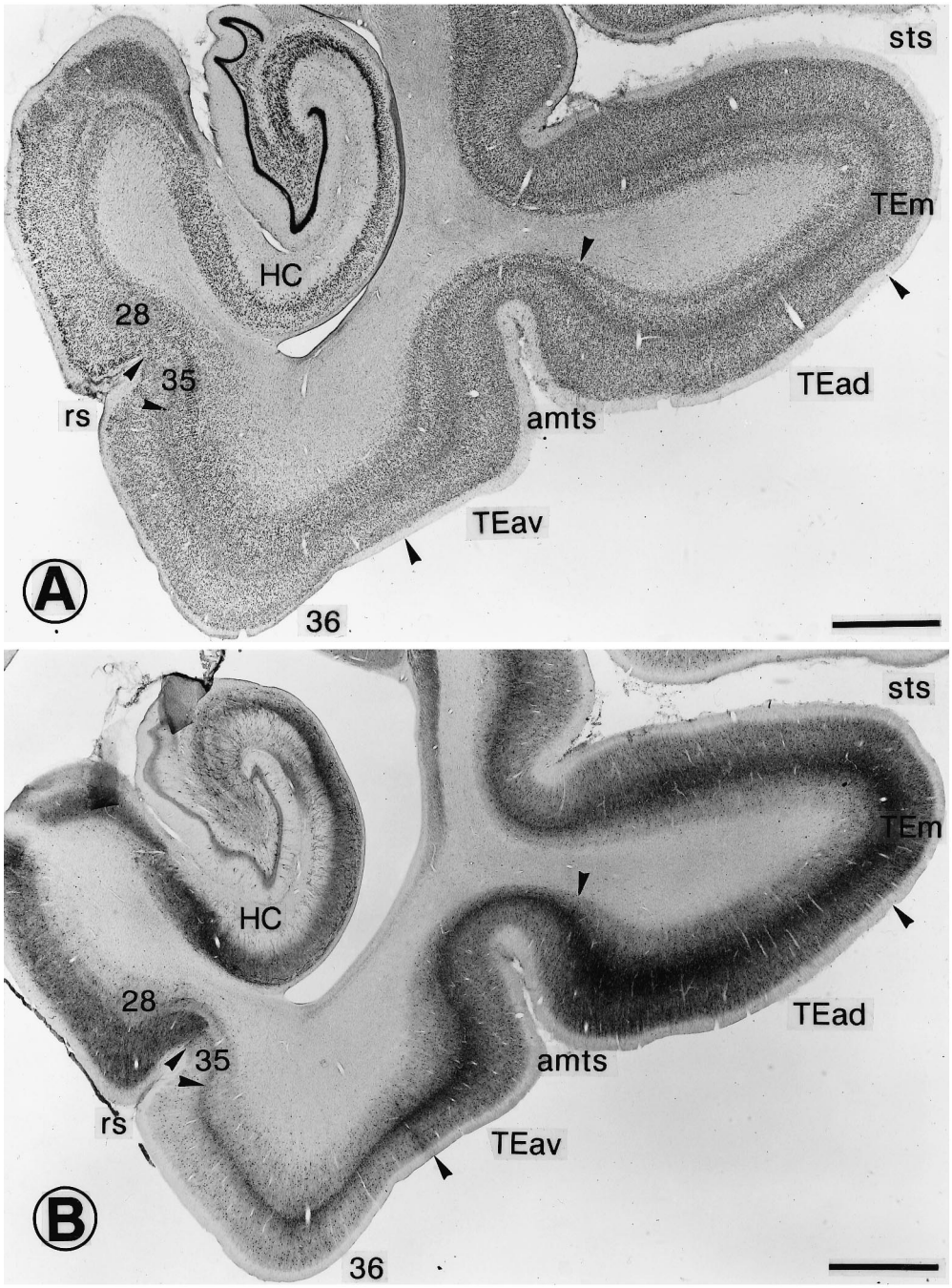

Figure 2. Cytoarchitectonic subdivision of anterior TE, perirhinal cortex, and the entorhinal cortex. *A*, Nissl-stained coronal section. The *arrowheads* indicate the borders between different areas. There is a clear distinction between layers IV, V, and VI in *TEad*, but it is less prominent in *TEav*. *B*, Adjacent section stained immunohistochemically for parvalbumin. There is a clear decrease in the density of immunostaining at the border from *TEav* to area *36*. Both neurons and neuropil are more lightly stained in area *36* than in *TEav*. The parvalbumin staining is even lighter in area *35*, but suddenly becomes dense at the border from area *35* to area *28*. Scale bars, 2 mm.

PHA-L was injected iontophoretically (Midgard precision current source, Stoelting), according to the procedure recommended by Gerfen and Sawchenko (1984) with some modifications. A glass micropipette with a 30–35 μm inner tip diameter was filled with 2.5% PHA-L (Vector Laboratories, Burlingame, CA) dissolved in Tris buffer (pH 7.4, 37°C). The micropipette was attached to the manipulator and was aligned normal to the cortical surface. The tip of the pipette was advanced first into the cortex by 2 mm, and then withdrawn to an appropriate depth (between 0.8 and 1.2 mm from the surface). PHA-L was injected with pulsed currents (7 μA, tip-positive, 7 sec on/7 sec off) for 20–25 min.

Biocytin (4%, Sigma, St. Louis, MO) dissolved in Tris buffer (pH 7.8) was injected iontophoretically as in the case of the PHA-L injections. WGA-HRP was injected by pressure. A glass micropipette (40–50 μm inner tip diameter) was attached to the tip of a 1 μl Hamilton syringe and filled with WGA-HRP (5%, Toyobo, Japan) dissolved in 0.1 M phosphate buffer (pH 7.2–7.4). The tip of the pipette was advanced first into the cortex by 0.8–1.0 mm, and then 0.1–0.2 μl of WGA-HRP was delivered per injection site over 10 min. The pipette was left in the cortex for 5–10 min after the injection to minimize leakage of the tracer from the injection site.

Histological processing. The survival period after the injection was 16–18 d in the PHA-L cases and 2 d in both the biocytin and the

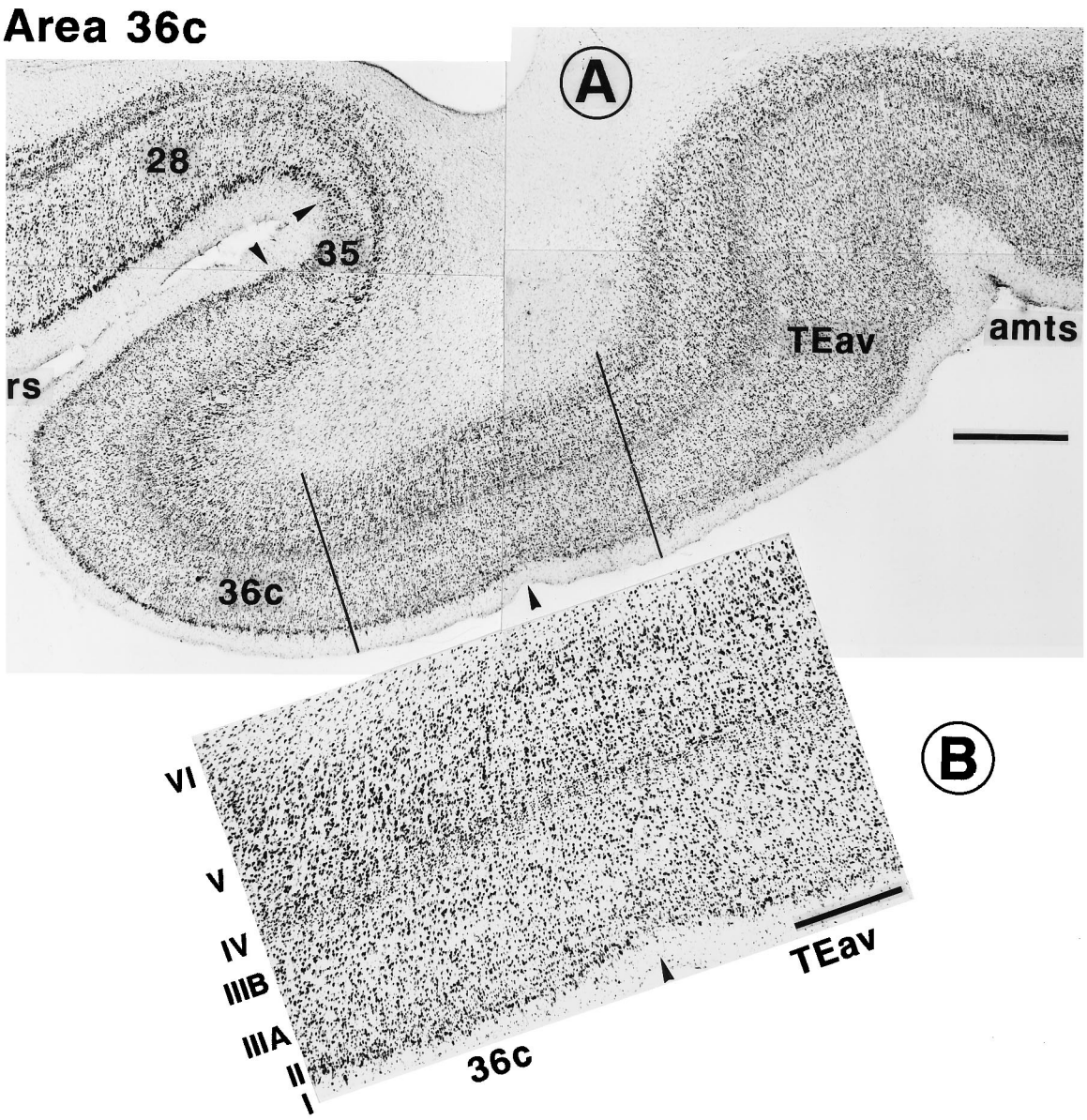

Figure 3. Cytoarchitecture of TEav, the caudal part of area 36 (36c), area 35, and area 28. *A*, Nissl-stained section. There is a separation between layers V and VI in *TEav* but not in *36c*. Layer IV is present in area 36 but absent in areas *35* and *28*. The presence of intensely stained large neurons in layer II distinguishes area *28* from area *35*. *B*, A part of *TEav* and *36c*, between the two parallel lines in *A*, is shown at higher magnification. *Roman numerals* indicate the cortical layers. The distinction between *IIIA* and *IIIB* is obvious in *36c*, but not in *TEav*. Similarly, densely stained large pyramidal neurons in layer *V* are more numerous in *36c* than in *TEav*. Scale bars: *A*, 1 mm; *B*, 0.5 mm. All other conventions are as in Figure 1.

WGA-HRP cases. The monkey was anesthetized with a lethal dose of sodium pentobarbital (60–80 mg/kg, i.v.) and perfused transcardially with 1 l of 0.9% warm heparinized saline, then 3–4 l of 4% paraformaldehyde in 0.1 M phosphate buffer (pH 7.2–7.4), 1–2 l of 10% sucrose in 0.1 M phosphate buffer and, finally, 1 l of 20% sucrose in 0.1 M phosphate buffer. The flow rate of the fixative solution was adjusted so that the perfusion with paraformaldehyde took 30–45 min. The brain was removed immediately after the perfusion. Photographs of different views of brain were taken, and the brain was blocked and then placed in 30% buffered sucrose at 4°C until it sank. Frozen sections were cut in the frontal plane at 30 or 40 μm thickness in the PHA-L cases and 50 μm thickness in both the biocytin and the WGA-HRP cases. Sections were collected in 0.05 M Tris-buffered saline (TBS) in the PHA-L cases and in 0.1 M phosphate buffer in the biocytin and WGA-HRP cases. All sections were processed in the PHA-L cases, but a series of every fifth section was processed in the biocytin and WGA-HRP cases. The remaining sections in the latter cases were processed for Nissl and parvalbumin staining to determine the borders of the cortical areas and the layer borders. It has been found recently that the parvalbumin staining in the perirhinal cortex is much sparser than that in the surrounding regions (Kondo et al., 1994).

Transported PHA-L was visualized by the same procedure as that described by Saleem et al. (1993b). The HRP reaction was carried out according to the modified tetramethyl benzidine method described by Gibson et al. (1984). For biocytin, we used a modified protocol of Lachica et al. (1991).

The quality of PHA-L labeling was equally good in two TEav cases (see Fig. 7*A*,*B*) and one TEad case (see Fig. 8*A*). The labeled profiles were clear in both gray matter and white matter, and the labeling was clear even in the cortical areas far from the injection site, for example, the prefrontal cortex. In the other TEad case (see Fig. 8*B*), there was no PHA-L labeling in the prefrontal cortex, and even in the perirhinal cortex the labeling in the white matter was less prominent than those in the other cases.

Data analysis. The sections were observed with a light microscope under bright- and dark-field illumination. To examine the global distribution of labeling, labeled terminals and neurons in TE and the perirhinal

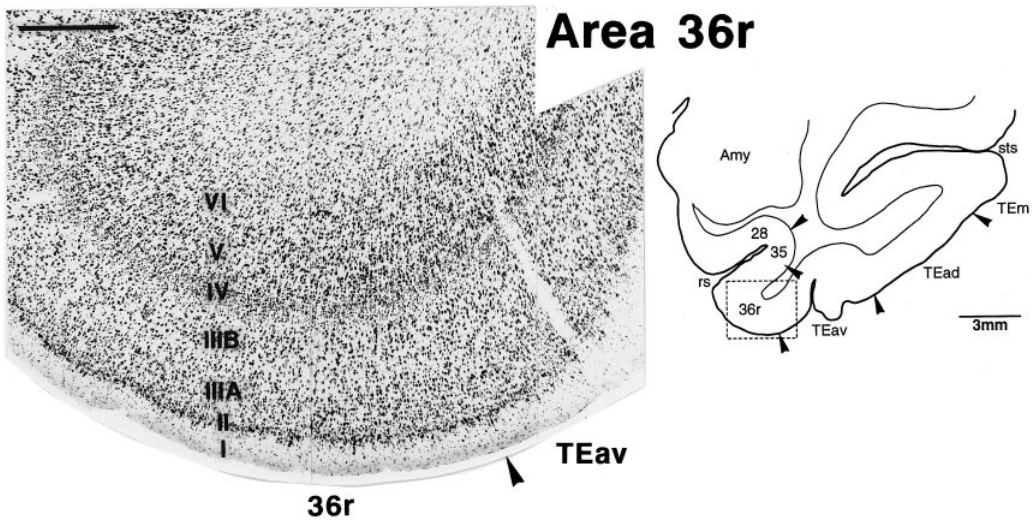

Figure 4. Cytoarchitecture of TEav and the rostral part of area 36 (36r) in a Nissl-stained section. The position of the photomicrograph is indicated by the *box* in the lower-magnification line drawing of the section on the *right*. The subdivision of layer III into *IIIA* and *IIIB* is clearer in 36r than in 36c (Fig. 3), and layer *II* is more distinctive with many darkly stained neurons and satellite glial cells in 36r. Such distinction is not clear in TEav. Scale bar, 0.5 mm.

and entorhinal cortices were plotted first onto enlarged camera lucida drawings of sections, which were transformed into two-dimensional unfolded maps of the cortical regions. Sections were sampled for this purpose at 0.5 mm intervals. If the labeling was very sparse, the sampling interval was decreased to 0.25 mm. Layer IV and cytoarchitectonic borders between the areas were traced from the adjacent thionin- and parvalbumin-stained sections. The layer IV contour lines of the sampled sections were straightened and arranged in parallel to produce a two-dimensional unfolded map of anterior TE and the perirhinal and entorhinal cortices (Fig. 1, *top right*). The fundus of the rhinal sulcus was used as a reference point in the arrangement, i.e., sections were aligned along the shape of the rhinal sulcus taken from the picture of the ventral view of the brain (Fig. 1, *top left*). The length of the contour lines was not changed and, thus, the distortion is minimal around the rhinal sulcus and is larger at positions near the superior temporal sulcus. The flattened maps covered cortical regions up to the ventral lip of the superior temporal sulcus laterally, and to the medial border of the entorhinal cortex medially (indicated by *shaded regions* in Fig. 1, *bottom*).

Single axons were reconstructed from serial PHA-L sections, which were aligned with blood vessels and other labeled axons in the vicinity of the axon whose course was being traced. Individual axons were reconstructed with a camera lucida and 20× or 40× objectives. Some of the PHA-L sections were Nissl-stained after the PHA-L observation was completed to determine the borders of the cortical areas and the layer borders.

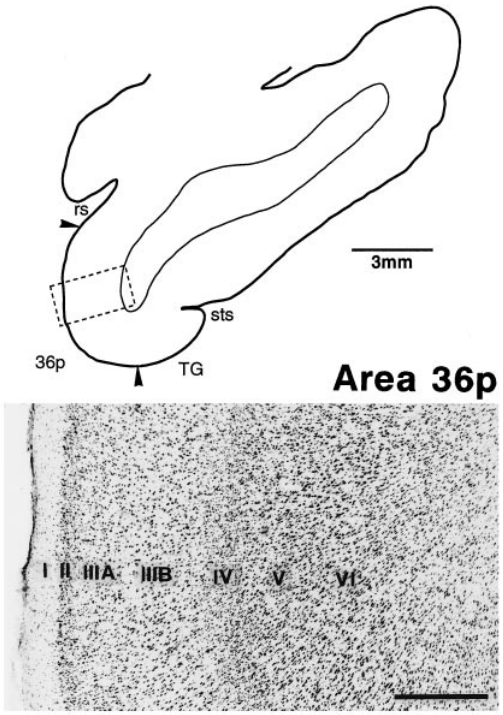

Figure 5. Cytoarchitecture of the polar part of area 36 (36p) in a Nissl-stained section. The position of the photomicrograph is indicated by the *box* in the line drawing of the section at the top. The distinction between *IIIA* and *IIIB*, and that between *V* and *VI*, is not clear. Also, layer *IV* is less distinctive than those in 36c and 36r. Scale bar, 0.5 mm.

RESULTS

Injections of anterograde tracers into TEav and TEad resulted in heavy labeling of axon terminals in area 36 of the perirhinal cortex in both cases, less dense but definite labeling in areas 35 and 28 in the TEav-injection cases, and some labeling in TG (the dorsal half of the temporal pole) in both cases. There was also heavy labeling of terminals in the anterior part of the superior temporal sulcus and mutual projections between TEav and TEad, both of which will be described in other papers. There were sparsely labeled terminals in the parahippocampal gyrus (TF/TH) after the TEad injections, but not after the TEav injections.

The positions of the borders between different cortical areas will be described first, because they are crucial in interpreting the results regarding connections. There are three main points for the borders: (1) the border between the dorsal and ventral parts of anterior TE (TEad and TEav, respectively); (2) the border between TEav and the perirhinal cortex; and (3) the rostrocaudal extent and subdivision of the perirhinal cortex.

The border between TEad and TEav

Brodmann (1905) divided the inferotemporal region corresponding to TE into area 21 (dorsal) and area 20 (ventral). The border between these two regions was located at the anterior middle temporal sulcus (amts). Yukie, Iwai, and their colleagues (Iwai and Yukie, 1987, 1988; Iwai et al., 1987; Yukie and Iwai, 1988; Yukie et al., 1990) found that the dorsal and ventral parts of TE,

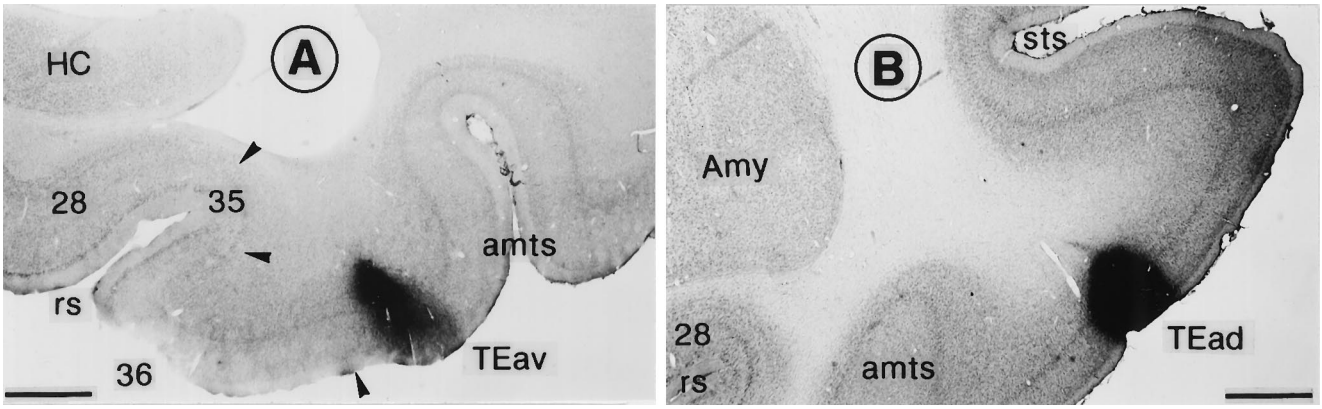

Figure 6. Photomicrographs illustrating the PHA-L injection sites in TEav (*A*) and TEad (*B*). Sections were counterstained for Nissl. Injections in both cases involved all of the cortical layers. Scale bars, 1 mm. All conventions are as in Figure 1.

which roughly corresponded to Brodmann's areas 21 and 20, have differential connections with the amygdala and hippocampus. Based on this dorsal versus ventral TE difference as well as the previously reported posterior versus anterior TE difference in the afferent connection from the prelunate gyrus (Shiwa, 1987; Morel and Bullier, 1990), Yukie and colleagues have divided TE into four subregions: TEpd (posterior–dorsal), TEpv (posterior–ventral), TEad (anterior–dorsal), and TEav (anterior–ventral).

We basically adopted the subdivision described by Yukie et al. (1990), but we found that the border between TEad and TEav described by Yukie et al. (1990) corresponds to the cytoarchitectural border between TE2 and TE1 described by Seltzer and Pandya (1978). We therefore used the cytoarchitectural criterion used by Seltzer and Pandya (1978) to determine the border between TEad and TEav: layer V is less populated by neurons in TEad than in TEav (Fig. 2*A*). The border thus determined was located at the lateral bank or lip of the amts at the rostrocaudal level and approached the superior temporal sulcus (sts) as it continued further anteriorly (Figs. 1, 2). The lateral border of TEad was defined by the cytoarchitectural border between TE2 and TEm described by Seltzer and Pandya (1978) (Figs. 1, 2). The border of TEav with TG was less clear than the other borders, but it is not essential to the present results (Fig. 1, *dashed line*).

The border between TEav and the perirhinal cortex

Our definition of the border between TEav and the perirhinal cortex is similar to that of Amaral and colleagues (Amaral et al., 1987; Suzuki and Amaral, 1994a,b). There was a clear separation between layers V and VI in TEav but not in area 36 (Figs. 2*A*, 3), differentiation of layer III into IIIA and IIIB was clearer in area 36 than in TEav (Fig. 3), and the proportion of densely stained large pyramidal cells in layer V was greater in area 36 than in TEav (Fig. 3). In addition, we found that in the sections stained immunohistochemically for parvalbumin there was a clear decrease in the density of staining at the border from TEav to area 36. The staining of both neurons and neuropil was lighter in area 36 than in TEav (Fig. 2*B*).

The border between TEav and area 36 determined by the above described criteria was located at a position one-third to one-half the distance from the medial lip of the amts toward the lateral lip of the rhinal sulcus at the caudal part corresponding to the caudal end of the rhinal sulcus, and it ran rostrally roughly parallel to the rhinal sulcus (Fig. 1). In most cases in which the amts curved medially at its rostral end, the border was located at the medial lip of the rostral end of the amts. There seems to be a species difference. The border determined here in the Japanese monkeys was located more medially than that determined by the Amaral group in cynomolgus monkeys (Fig. 1 of Suzuki and Amaral, 1994a; Fig. 3 of Suzuki and Amaral, 1994b). The location of the border determined by other groups in rhesus monkeys was similar to that determined by us in Japanese monkeys (Meunier et al., 1993; Gaffan, 1994).

Amaral et al. (1987) divided the perirhinal cortex into areas 36 and 35. We followed their subdivision and used the same criteria to determine the border between areas 36 and 35: there was no layer IV in area 35, whereas it was present in area 36 as in the neocortical areas (Fig. 3*A*). The mediolateral extent of area 36 may be divided further into subregions, as suggested by Van Hoesen and Pandya (1975a), and the present results of differential projection from TEav and TEad partially support such subdivision. We indicate the entire mediolateral extent as area 36 in this paper for simplicity.

To determine the border between area 35 and the entorhinal cortex (area 28), we used the abundance of large and densely stained neurons in layer II of area 28 (Figs. 2*A*, 3*A*), in accordance with previous studies [Amaral et al. (1987) and references therein]. We found that a discontinuity in parvalbumin staining coincided with the border. There were many parvalbumin-immunoreactive neurons in layers II and III of area 28, whereas there were few or were absent in layers II and III of area 35 (Fig. 2*B*).

Rostrocaudal extent and subdivision of the perirhinal cortex

The temporal pole was referred to previously as TG (von Bonin and Bailey, 1947) and discriminated from the perirhinal cortex. In the present study, the projection from TEav and TEad to the perirhinal cortex continued to the ventromedial aspect of the temporal pole, but not to the dorsolateral aspect. We therefore decided to include the ventromedial aspect of the temporal pole in the perirhinal cortex, and refer to it as 36p (polar), but we exclude the dorsolateral aspect. The caudal border of the perirhinal cortex was situated at the caudal end of the rhinal sulcus, because the projection from TEav and TEad terminated at this level. It roughly corresponded to the position of the cytoarchitectural changes described in previous studies for this border (Amaral et al., 1987; Suzuki and Amaral, 1994a).

To facilitate the description of rostrocaudal positions of the labeled terminals, we divided area 36 into three subdivisions

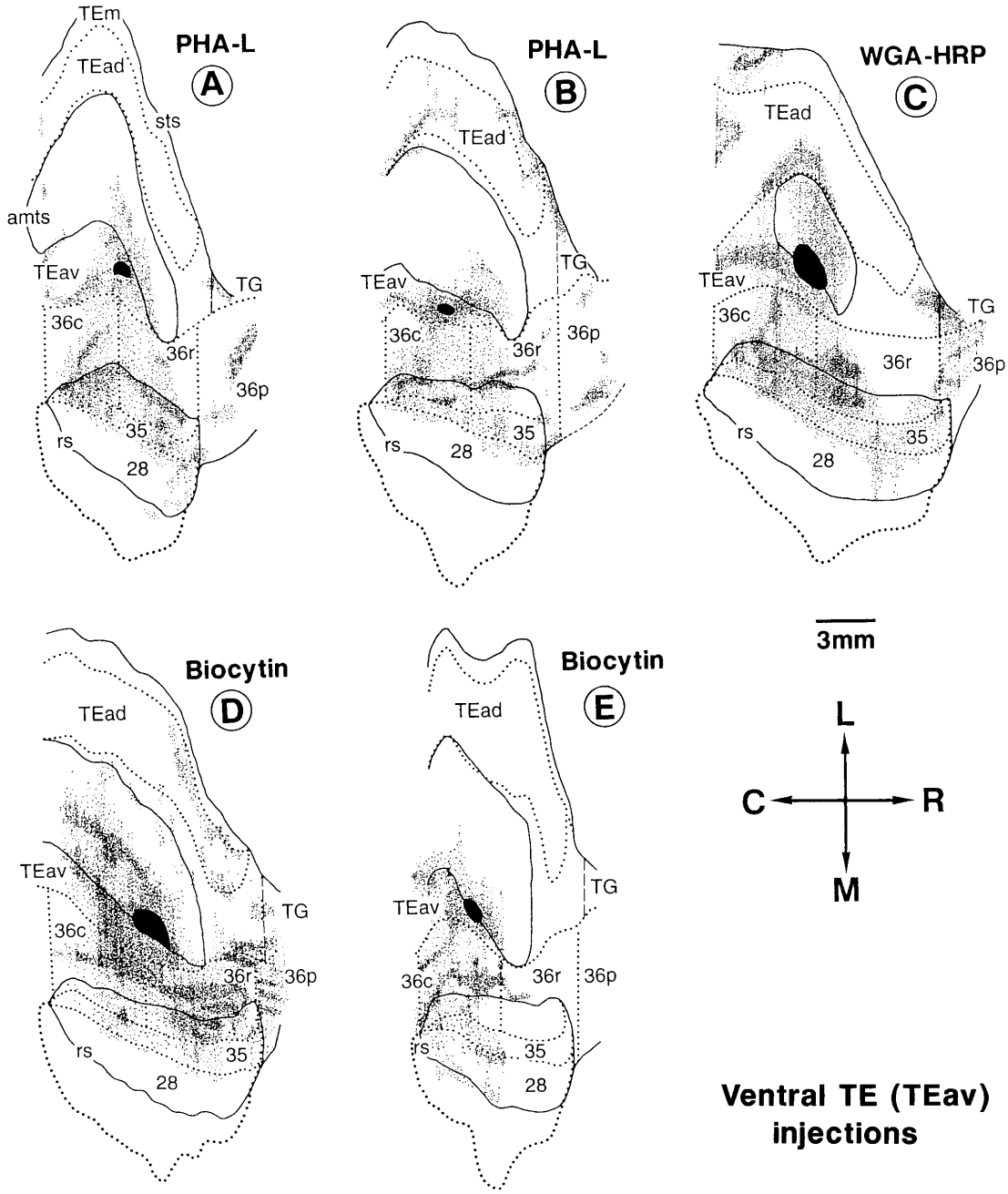

Figure 7. Distribution of anterogradely labeled terminals after PHA-L, biocytin, and WGA-HRP injections into TEav. The *filled region* indicates the extent of the injection site, and the *small dots* at different densities represent the terminal labeling. All other conventions are as in Figure 1.

following Insausti et al. (1987). The most rostral part, which previously was named TG, is referred to as 36p (polar), the middle part as 36r (rostral), and the caudal part as 36c (caudal). The subdivision of layer III into IIIA and IIIB was clearer in 36r than in 36c and 36p; layer II was more distinctive with densely packed, darkly stained neurons and satellite glial cells in 36r and 36p than in 36c; layer IV is less distinctive in 36p than in 36r and 36c; and, finally, the border between layers V and VI was less clear in 36p than in 36r and 36c (Figs. 3–5). The borders between these subdivisions of area 36 were less clear than the borders of area 36 with the surrounding regions. Our 36p corresponds to 36pm of Insausti et al. (1987). Recently, Suzuki and Amaral (1994a) modified the division described by Insausti et al. (1987), and their new 36r included both our 36r and 36p.

Injection sites

The injection sites were well localized within TEad or TEav, and none of the injection sites including the rather large ones of WGA-HRP crossed the border between TEad and TEav or that between TEav and area 36 (Figs. 6–8). The injection sites of PHA-L were localized to small foci, which were 0.5–1.0 mm in width in the plane parallel to the cortical layers and included all of the cortical layers (Fig. 6*A*,*B*). One case in which the PHA-L injection site was mostly limited to the deep layers was excluded

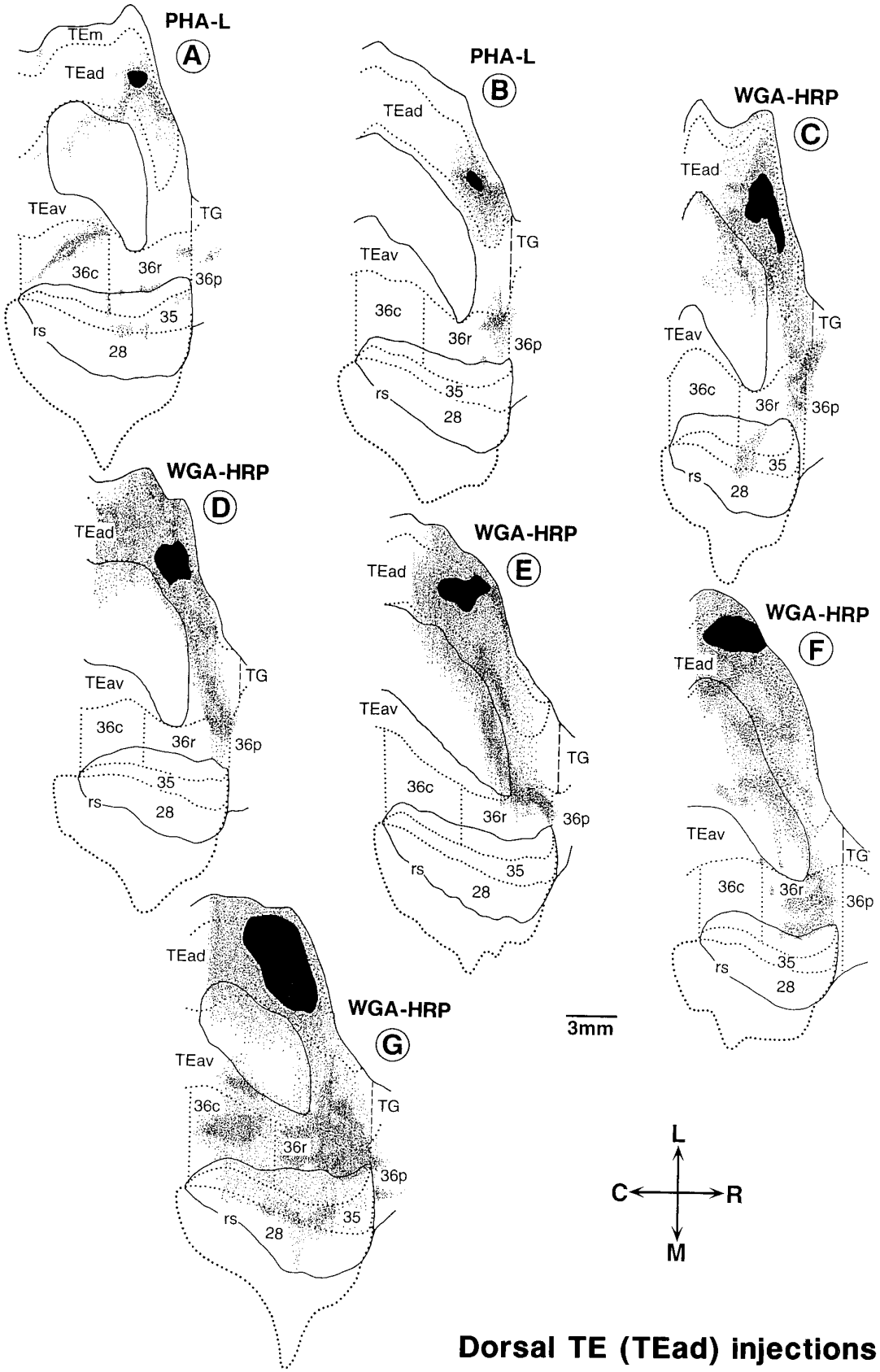

Figure 8. Distribution of anterogradely labeled terminals after PHA-L and WGA-HRP injections into TEad. The flattened map in one case (*F*), in which the injection was made in the left side, was reversed for convenience of comparison. All conventions are as in Figure 1.

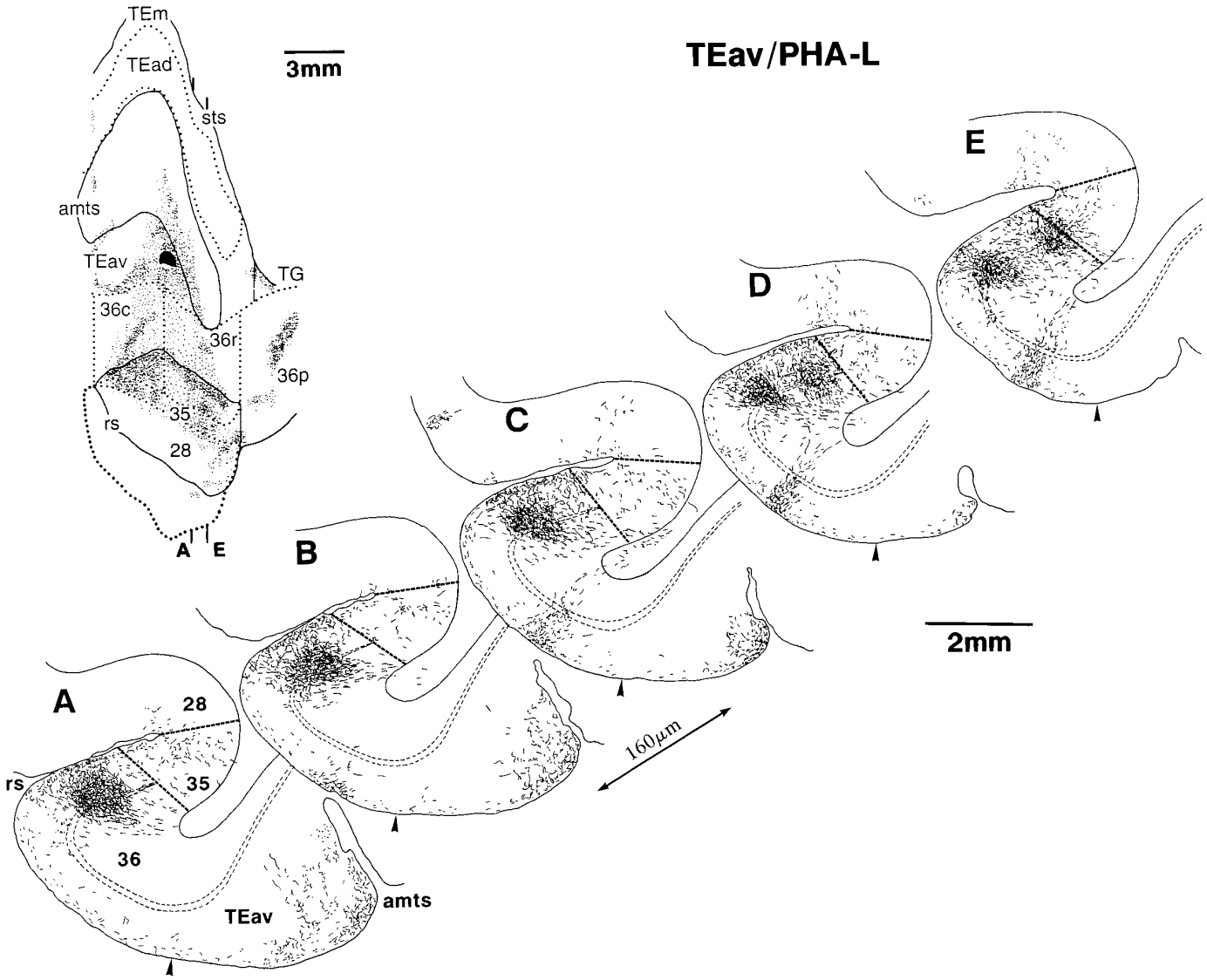

Figure 9. Caudorostrally elongated core regions and laminar distribution of terminals in area 36 after a PHA-L injection into TEav. A series of coronal sections at regular intervals of 160 μm is shown (*A–E*). The *inset* at the *top left* illustrates the rostrocaudal levels of these sections on the same drawing as shown in Figure 7*A*.

from the present analysis. The biocytin injection sites were 1.0–1.5 mm in width, and the WGA-HRP injection sites were larger (2.5–4.8 mm in width). The biocytin and WGA-HRP injection sites also included all of the cortical layers.

Global distribution patterns of labeled terminals

The global distribution patterns of labeled terminals are shown in Figures 7 and 8 for all cases.

Both TEav and TEad strongly projected to area 36, but there were differences in distribution of labeled terminals between the two cases. Labeled terminals after the focal injections of PHA-L were more widely distributed in the TEav-injection cases than in the TEad cases. Also, the labeling tended to be biased to the medial part of area 36 in the TEav cases, whereas the labeling was more or less limited to the lateral part of area 36, avoiding the lateral bank of the rhinal sulcus in the TEad cases.

Labeled terminals were distributed widely both caudorostrally and mediolaterally in the perirhinal cortex after the focal injections of PHA-L into TEav. The distribution covered all of the caudorostral subregions of area 36, i.e., 36c, 36r, and 36p, except in one biocytin case in which 36p was spared (Fig. 7*E*). Although the distribution covered a large mediolateral part of area 36, there was a mediolateral gradation in density. The distribution of labeled terminals tended to be denser in the medial part and became sparser toward the lateral border (Fig. 7*A*,*B*). This mediolateral gradation was also observed in the WGA-HRP and biocytin cases (Fig. 7*C–E*). The rostral half of 36r was spared or only sparsely populated by the labeled terminals. This is of interest, because this region received denser projection in most of the TEad cases (Figs. 7, 8).

In the TEav cases, labeled terminals were also distributed throughout the caudorostral extent of area 35 of the perirhinal cortex and the entorhinal cortex (area 28), although the labeling in area 28 was mostly limited to the lateral part along the medial bank of the rhinal sulcus (Figs. 7, 9). The distribution of labeled terminals in area 35 was as dense as that in area 36, but that in area 28 was sparser. The amount of labeling in area 28 also varied between the TEav cases.

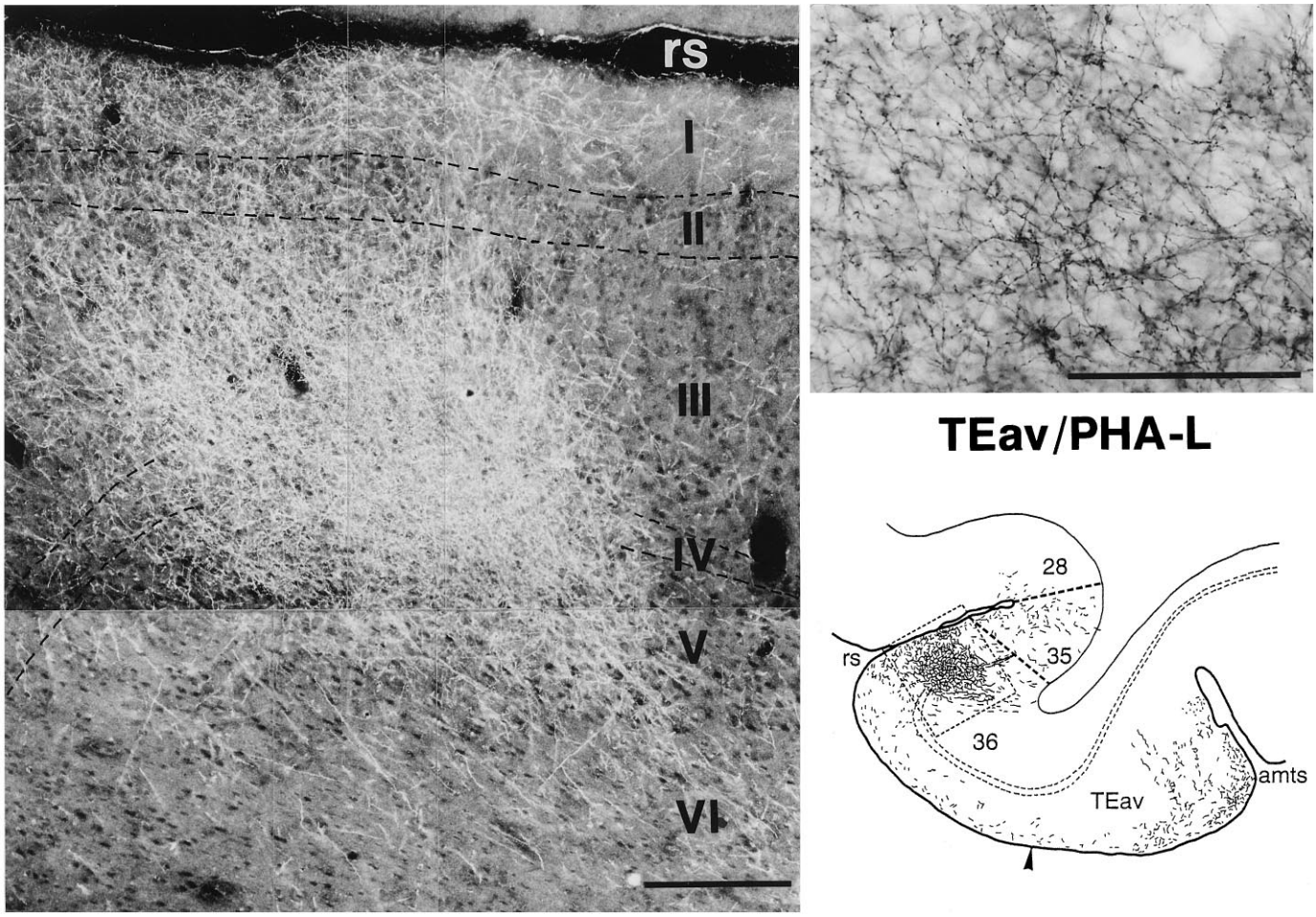

Figure 10. Dark-field photomicrograph of a dense core region in area 36, which is illustrated at the *bottom right* within the circumscribed area (same as Fig. 9*A*). The high-magnification photomicrograph of terminals with boutons (bright-field) at the *top right* is taken from layer III of the photomicrograph shown at the *left*. Scale bars: *left*, 0.25 mm; *right*, 0.1 mm.

After injections into TEad, labeled terminals were confined to smaller regions than those after TEav injections, except in the WGA-HRP case with the largest injection site (Fig. 8*G*). The labeled region was located at the rostrolateral part of 36r in 4 of 7 cases (Fig. 8*B–E*), at the middle of 36r in one case (Fig. 8*F*) and at the lateral part of 36c in the remaining case (Fig. 8*A*). There was virtually no labeling or much sparser labeling in the medial part of area 36, located at the lateral bank of the rhinal sulcus. Because the caudorostral position of the injection sites varied among the four cases in which terminals were predominantly found in the rostrolateral part of 36r, it may be concluded that the projections from different caudorostral sites of TEad converge in the rostrolateral part of 36r. In the WGA-HRP case with the largest injection site (Fig. 8*G*), the distribution of labeled terminals covered a wide region of area 36 including all of the foci labeled in the other TEad cases (Fig. 8*A–F*).

A complementary pattern of projections from TEav and TEad to area 36 was observed in one of the two cases in which injection of WGA-HRP into TEad was combined with that of biocytin into TEav in the same hemisphere (see Figs. 7*D*, 8*E*). Projection from TEav was sparser in the rostrolateral part of 36r than the other subregions in area 36, and the dense and mostly confined projection from TEad was found in the same rostrolateral part of 36r (compare Figs. 7*D*, 8*E*). In another case with combined injections, the complementary pattern was not revealed because projections from TEav and TEad were not overlapped caudorostrally (compare Figs. 7*E*, 8*C*).

Labeled terminals were found in area 35 in 3 of the 7 TEad cases (Fig. 8*A*,*C*,*G*). Labeling in area 28 was present, but very scattered, in the same three cases. No labeling in areas 35 and 28 was observed in the other four TEad cases.

Caudorostrally elongated core regions and laminar distribution of terminals

In the distribution of labeled terminals in area 36, there were regions with denser labeled terminals. These dense terminal regions were clearly delineated from the surrounding region with less dense terminals. We call these dense terminal regions as "core regions." The core regions were elongated in the caudorostral direction, and in the frontal sections they appeared to compose columnar regions (0.2–0.85 mm in width) extending across the cortical layers (Figs. 9–11). The labeled terminals were most densely distributed in the middle layers from layer III to the upper part of layer V and in layer I (Figs. 9–11). The distribution of labeled terminals in layer II and layer VI tended to be sparser.

There were three to eight separate core regions in each of the TEav cases, and one to three core regions in each of the TEad

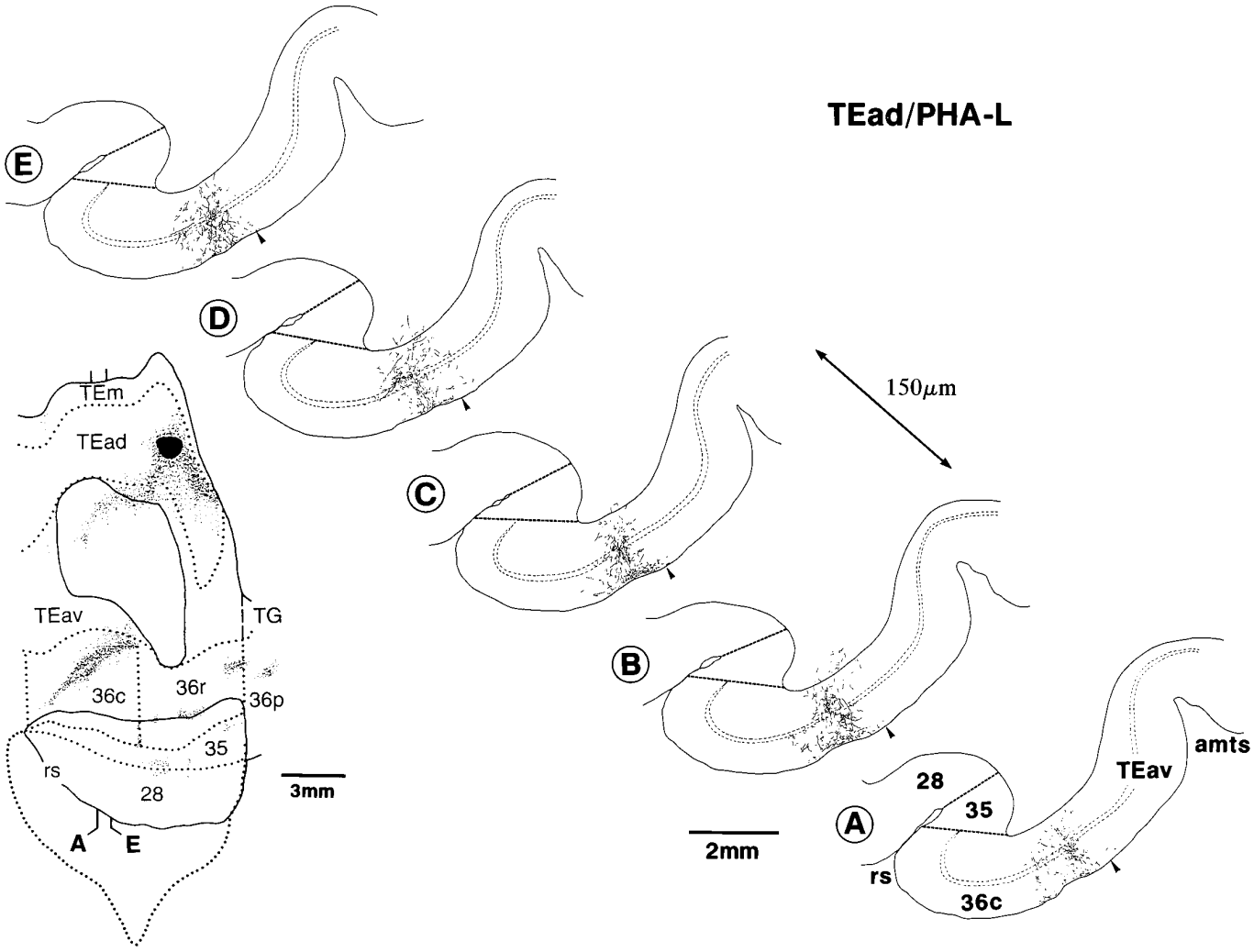

Figure 11. Caudorostrally elongated core regions and laminar distribution of terminals in area 36 after a PHA-L injection into TEad. A series of coronal sections at regular intervals of 150 μm is shown (*A–E*). The figure on the *left* illustrates the rostrocaudal levels of these sections on the same drawing as shown in Figure 8*A*.

cases. The length of the core regions in the caudorostral direction varied from 1.5 to 4.5 mm. The laminar distribution of labeled terminals in the surrounding regions was different from that in the core regions. Just outside the core regions, the densest distribution in the middle layer tended to be reduced in width to narrower bands in and around layer IV, whereas the labeling in layer I continued (Figs. 9, 17). Far from the core regions, labeled terminals were sparsely distributed in all layers (Fig. 9).

The core regions were found in area 36 as described above, but there were no clear core regions in areas 35 and 28. Labeled terminals were found in all of the cortical layers in areas 35 and 28 (Fig. 9).

Reconstructed single axons

To investigate how the overall distributions of labeled terminals, especially those of core regions that encompassed all the cortical layers, were composed of single axons, we reconstructed single axons from serial sections in the PHA-L cases. Most of our reconstruction was made from the core regions in the TEad case (shown in Fig. 8*A*), but not in the TEav cases, because the core regions in the TEav cases were too dense for single-axon reconstruction. Nine axons were reconstructed, eight from 36c and one from 36r. They were near fully reconstructed in the gray matter, except some of very thin branches that could not be followed among dense terminals of other axons. Their main axon trunks were followed toward the injection site in the white matter by >1 mm.

The reconstructed axons had one to six arbors, most of which were elongated vertically from layer VI, V, or IV to layer I or II (Figs. 12, 13), but all of the four distinctive arbors of one axon were limited to the superficial layers (layers I–III) (Fig. 14). There were no axons with arbors limited to the middle layers (in and around layer IV). The individual arbors varied in size but typically measured 150–500 μm caudorostrally and 180–615 μm mediolaterally. Detailed descriptions of three illustrated axons (Figs. 12–14) are given in the figure legends.

Retrogradely labeled neurons

In the WGA-HRP cases, both retrograde labeling of neurons and the anterograde labeling of axon terminals were found in the perirhinal and entorhinal cortices. The distribution of labeled neurons essentially coincided with that of labeled terminals in individual TEav and TEad cases. However, the distribution of labeled neurons extended more medially, beyond the medial limit

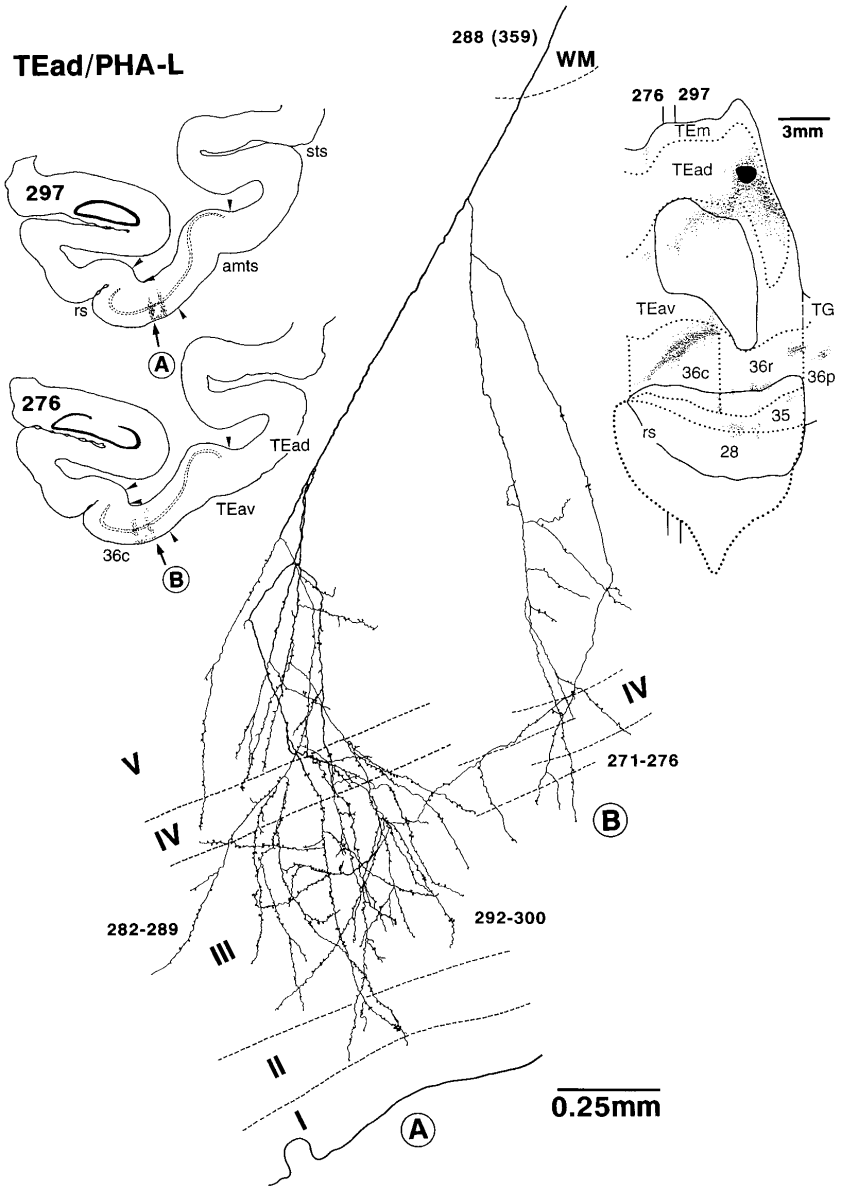

Figure 12. Single axon projecting from TEad to area 36c. It was reconstructed from serial PHA-L-labeled sections of the TEad-injection case shown in Figure 8*A*. The *numbers* indicate the serial numbers of individual sections (30 μm thickness) counted from caudal to rostral. The global positions of the arbors are shown in low-magnification drawings of two sections on the *left*. *Arrowheads* indicate the borders between different areas. The rostrocaudal levels of the two sections are indicated on the flattened map of the brain shown at the *top right*. This axon had two main branches, and the overall caudorostral extent of the arbors was 0.87 mm (271–300). The left branch had two arbors (282–289 and 292–300), which were located in the left core region indicated by "A" in the low-magnification drawing of section *297*. The terminal arbors were elongated vertically to the cortical layers expanding from layer VI to layer I. The right branch had one arbor (271–276) located in the right core region indicated by "B" in the low-magnification drawing of section *276*. The terminals were distributed from layer VI to layer III. The main axon trunk ran into the white matter (*WM*) and approached the injection site. All other conventions are as in Figure 1.

of the distribution of labeled terminals. In the TEav cases, the labeled neurons extended to the medial portion of the entorhinal cortex, where the labeled terminals were mostly absent (Fig. 15, *bottom*, sections *68*, *76*). Similarly, in the TEad cases, labeled neurons extended to the medial border of area 36 at some caudorostral levels, where the labeled terminals were mostly absent [Figs. 16 (*bottom right*, sections *88*, *92*), 17].

The labeled neurons were located in both the upper layers (layers II and III) and the deeper layers (layers V and VI) in area 36, but the labeled neurons in the deeper layers were more numerous than those in the upper layers, and at some locations the labeled neurons were limited to the deeper layers (Figs. 15, 16). The labeled neurons in areas 35 and 28 in the TEav cases were mostly limited to the deeper layers (Fig. 15, sections *68–84*).

DISCUSSION

Differential projection of TEav and TEad

Previous anatomical findings have shown differences between TEav and TEad in their afferent and efferent connections. TEav receives projections from the ventral part of TEO, whereas TEad receives projections from the dorsolateral part of TEO (Desimone et al., 1980; Martin-Elkins and Horel, 1992; Yukie et al., 1992). Their patterns of projection to the amygdala (Iwai et al., 1987) and the prefrontal cortex (Saleem et al., 1995) were also different. The present findings indicate that there are also differences in their connections with the perirhinal and entorhinal cortices (Fig. 18). A single site in TEav projects to a large part (approximately one-half of its total extent) of area 36 of the perirhinal cortex, whereas a single site in TEad projects to a rather small region of area 36 (less than one-tenth of its total extent), in most cases at the rostrolateral part of 36r. Projections to area 35 of the perirhinal cortex and the entorhinal cortex (area 28) were more numerous from TEav than those from TEad.

Our observation of the divergent projections from TEav is consistent with the conclusion of Suzuki and Amaral (1994b) that the medial part of TE (corresponding to our TEav and the medial part of TEad) projects divergently to all of the portions of the perirhinal cortex. They concluded this by analyzing the distribu-

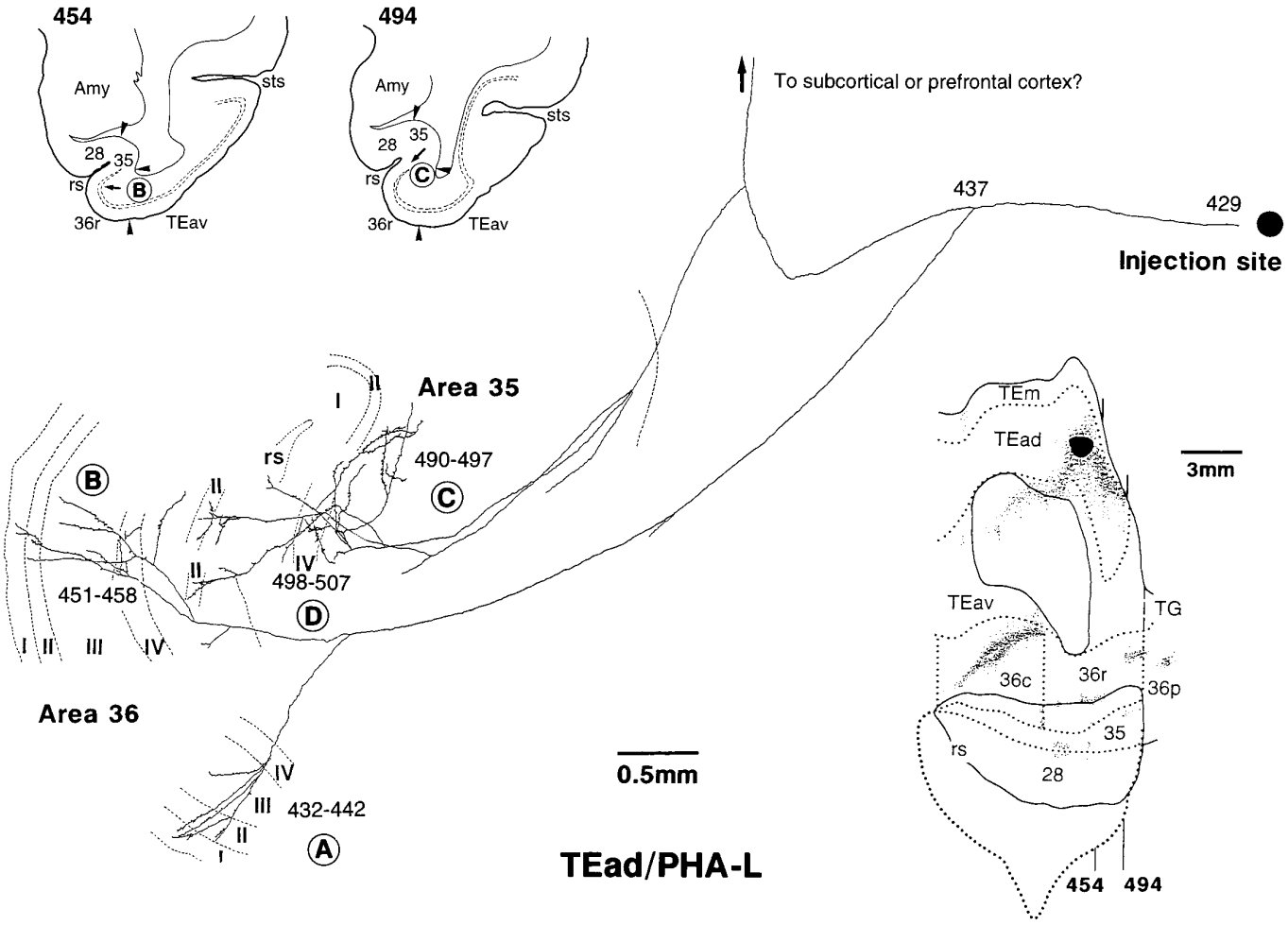

Figure 13. Single axon projecting from TEad to areas 36r and 35 reconstructed from the case shown in Figure 8*A*. This axon had three main branches. One branch was subdivided further into two arbors extending from layer V or IV to layer I (*A*, 432–442; *B*, 451–458). The position of the arbor marked by "B" is indicated by the *arrow* in the low-magnification drawing of section *454*. It was located at the lip of the rhinal sulcus in area 36r. The second branch had two arbors, one confined to layer III (*C*, 490–497) and the other extending from layer V to layer II (*D*, 498–507). Both were confined to area 35 in the fundus of the rhinal sulcus. The location of the arbor marked by "C" is shown by the *arrow* in the low-magnification drawing of section *494*. The third branch, which was not traced further, ran into the white matter toward other structures. The overall span of the arbors was 2.2 mm along the caudorostral axis (432–507).

tion of labeled neurons in different monkeys in which the retrograde tracers were injected into different subregions of the perirhinal cortex. The lack of labeled terminals in the medial part of area 36 located at the lateral bank of the rhinal sulcus observed in most of the TEad cases is consistent with the observation in adult monkeys by Webster et al. (1991) in their comparative studies of infant and adult monkeys.

There are two possible interpretations of the present results. One is that the perirhinal cortex receives visual inputs mainly from TEav and that the information from TEad goes to other brain sites. It has been found, for example, that the projection to the amygdala was stronger from TEad than from TEav (Iwai et al., 1987). The other possibility is that the perirhinal cortex is anatomically subdivided with regard to afferent inputs from TEav and TEad. We have found that the rostrolateral part of 36r receives strong projections from TEad, whereas the remaining parts of area 36 receive strong projections from TEav. The separate flow of visual object information in TE may continue to be separate in the perirhinal cortex. The separation of processing is, however, partial because the separation of projections from TEad and TEav was incomplete in area 36, and there were mutual projections between TEav and TEad (see Figs. 7, 8).

Differences in the global distribution of labeled terminals between individual cases were prominent in the TEad injection cases. After single injections, the labeled terminals were restricted in the rostrolateral part of 36r in four cases, whereas they were distributed over the middle part of 36r in one case and limited to lateral part of 36c in the last case. It is unlikely that these differences reflected the differences in projection pattern between different monkeys, because the largest injection of WGA-HRP in one case resulted in labeling of terminals in all of these subregions of 36. It is also unlikely that there is rough topographic organization for the projection from TEad to area 36, because the rostrocaudal levels of the injection sites in which the labeling was limited to the rostral 36r varied among cases, including the injection site in which the labeling was observed in 36c. It is more likely that different patchy regions in TEad project to different parts of area 36, but a majority of patches to the rostrolateral part of 36r and a minority to the middle part of 36r or 36c.

The global distribution pattern of labeled terminals was

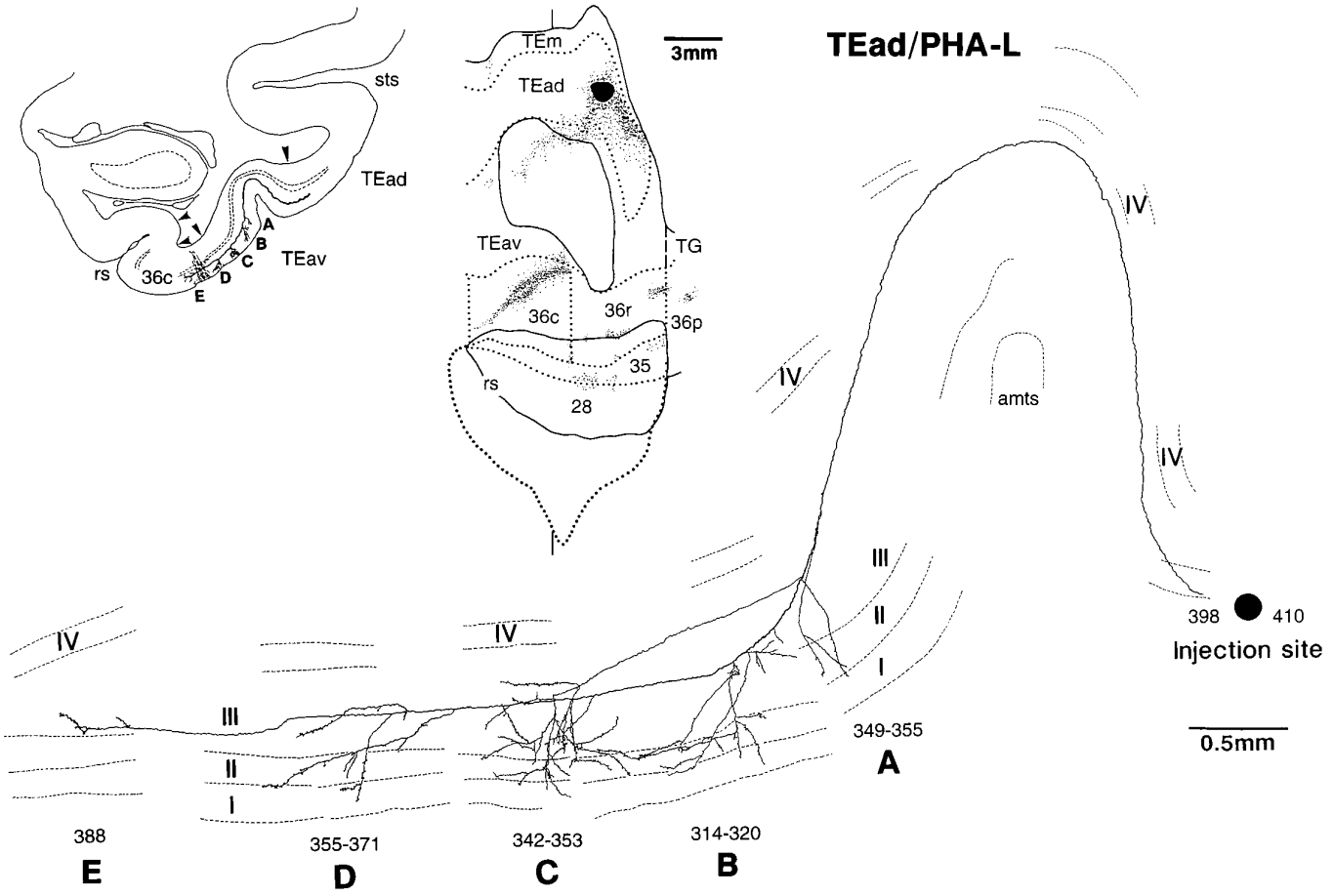

Figure 14. Single axon projecting from TEad to TEav and area 36c reconstructed from the case shown in Figure 8*A*. In contrast to Figures 12 and 13, the low-magnification drawing of the section at the *top left* schematically indicates the locations of the arbors, which actually appeared in different sections. This axon had five arbors, and they all extended from layer III to layer I, except one small arbor that was confined to layer III (*E*). The overall caudorostral extent of the arbors was 2.2 mm (314–388). Three of the arbors were located in TEav (*A–C*) and the others in the lateral portion of area 36c (*D*, *E*). The main axon trunk ran through the upper layers toward the injection site.

generally similar among the TEav cases. However, the positions of the core regions varied between individual TEav cases. This variation may be caused by the differences in the exact position of the injection sites, i.e., different patchy regions in TEav may project to different sets of patchy regions distributed over area 36. Similar, but less distributed, modular projections have been reported in the earlier stages of the ventral visual pathway (V2 to V4 and V4 to TEO) (Zeki and Shipp, 1989; Nakamura et al., 1993; DeYoe et al., 1994).

Association of visual features in the perirhinal cortex

That the divergent projection from TEav to the perirhinal cortex was found regardless of the position of the injection site in TEav indicates that a particular site in the perirhinal cortex receives convergent inputs from widely distributed sites in TEav. Such convergence may facilitate the association of different visual features. The importance of the perirhinal cortex for the association of different visual features has been suggested by the results of several lesion studies in the macaque monkey (Murray et al., 1993; Eacott et al., 1994; Gaffan, 1994). Also, by combining single-cell recordings from TE with lesions of the perirhinal and entorhinal cortices, Higuchi and Miyashita (1996) have found that the associative aspects of responses in TE depend on feedback connections from the perirhinal and entorhinal cortices.

The differences in the pattern of projections from TEav and TEad to the perirhinal cortex can be taken as cues to consider the functional difference between TEav and TEad. The information processed in TEav is expected to be more relevant to the associative function of the perirhinal cortex, although there are no available physiological data to support this hypothesis. The reported difference in afferent connections of TEav and TEad (Martin-Elkins and Horel, 1992; Yukie et al., 1992) suggests that cells in TEav have larger receptive fields than those of cells in TEad, because the peripheral visual fields are represented in the ventral part of TEO that projects to TEav and the central visual fields in the dorsolateral part of TEO, which projects to TEad (Boussoud et al., 1991). Horel (1996) proposed that "the details and colors of things but not global figures" are processed in TEad. Our recordings from TEad of the anesthetized monkeys showed that cells in TEad respond to both local and global features (Tanaka et al., 1991; Fujita et al., 1992; Ito et al., 1994, 1995; Kobatake and Tanaka, 1994). Responses of cells in TEav were too weak in anesthetized monkeys to examine extensively the size of receptive fields and response properties (H. Tamura and K. Tanaka, unpublished observations). Close comparison of cell responses between TEav and TEad in behaving monkeys is required to explore the functional difference between these two subareas of the inferotemporal cortex.

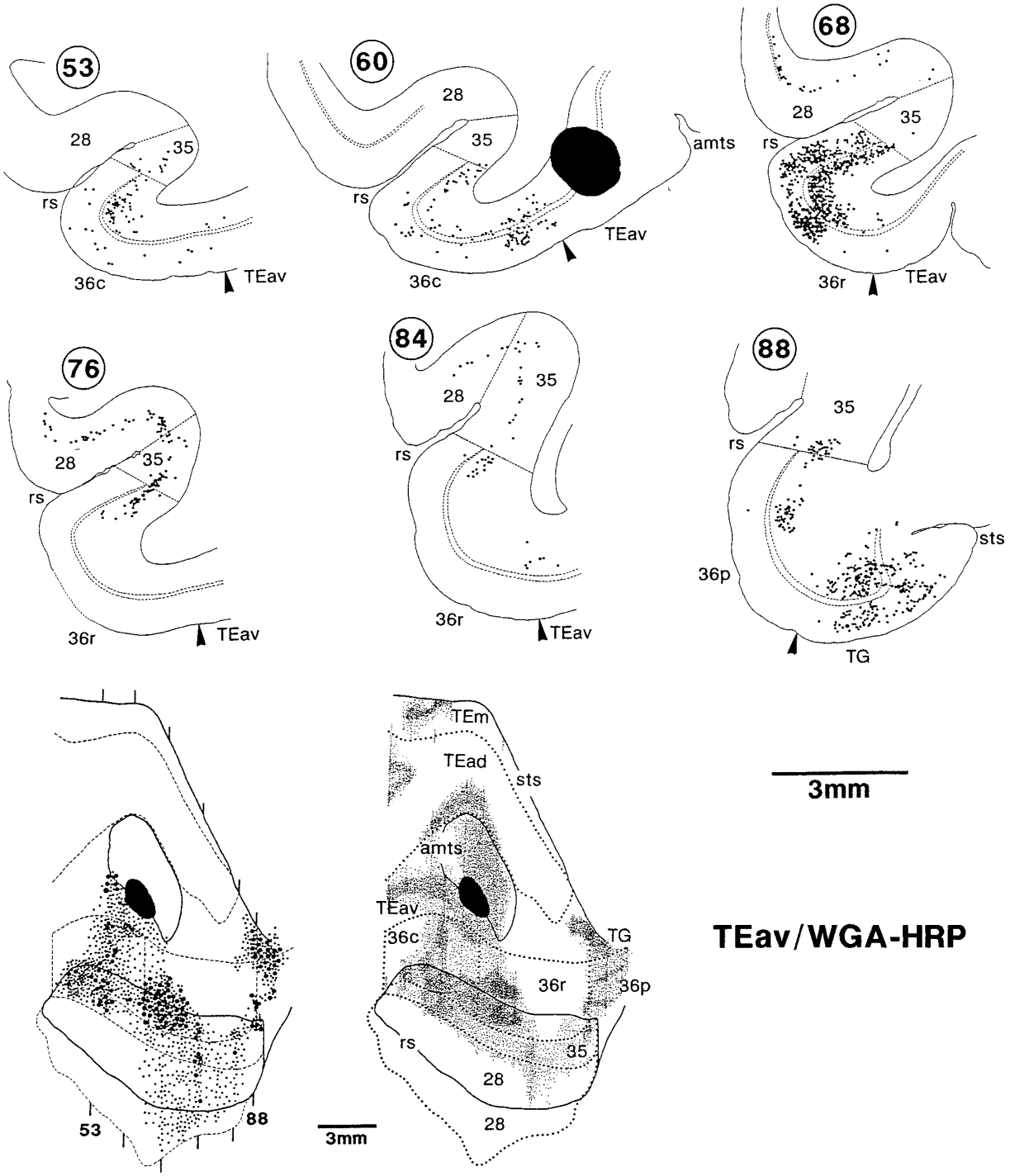

Figure 15. Distribution of retrogradely labeled neurons after WGA-HRP injection into TEav. *Top two rows*, A series of coronal sections, at intervals of 2 mm, in which the *filled region* indicates the injection site and the *dots* represent retrogradely labeled neurons. Only labeled neurons medial to the injection site are shown here and in the drawing shown at the *bottom left. Bottom left*, The global distribution of labeled neurons in the flattened map, in which a single *large dot* indicates a group of five neurons and *small dots* indicate single neurons. The positions of the coronal sections are also indicated. *Bottom right*, The global distribution of labeled terminals in the same case (the same drawing as Fig. 7*C*).

Laminar organization

The terminals of the projections from TE to area 36 were more densely distributed in the middle layers (from layer III to the upper part of layer V) and layer I, and cells that were the sources of the back-projections from area 36 to TE were more numerous in layers V and VI than in layers II and III. These properties of the connection between TE and area 36, when viewed from the side of TE, are closest to those of the feedforward type among the three proposed classes of cortico-cortical projections (Rockland and Pandya, 1979; Maunsell and Van Essen, 1983; Felleman and Van Essen, 1991). The TE-to-area 36 projection, however, differs from the typical feedforward cortico-cortical projections in that the terminals in the core regions were not limited to the middle layers but, rather, were distributed to all of the cortical layers, and

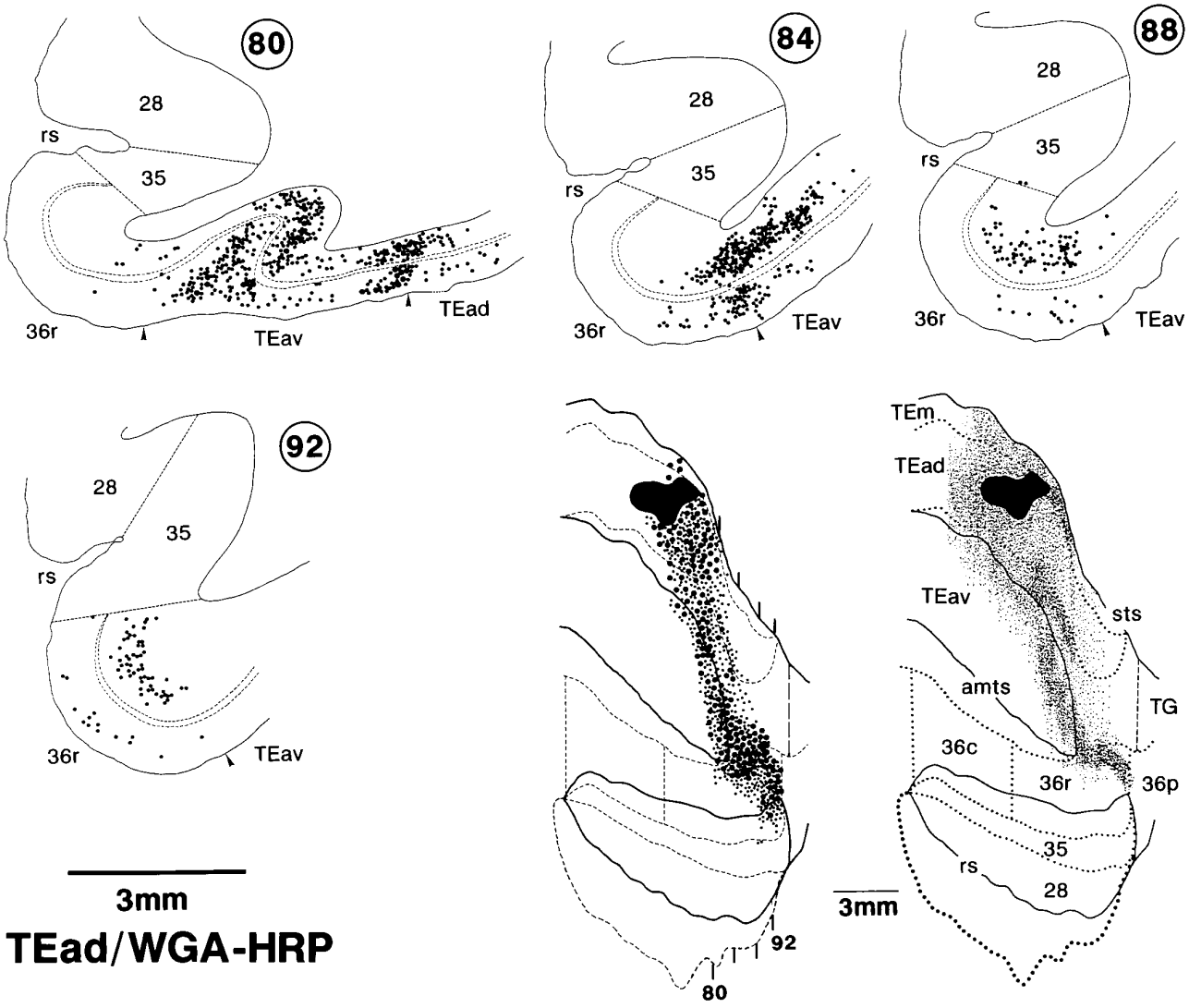

Figure 16. Distribution of retrogradely labeled neurons after WGA-HRP injection into TEad. A series of coronal sections, at regular intervals of 1 mm, with labeled neurons plotted as *dots* (*top* and *bottom left rows*), and also flattened maps showing the global distribution of labeled neurons (*bottom middle*) and terminals (*bottom right*). This is the same case as that shown in Figure 8*E*. Only labeled neurons medial to the injection site are shown in the coronal sections and in the flattened map.

terminals in layer I were as densely distributed as those in the middle layers.

The laminar distribution of terminals of the projection from TEO to TE was similar in general to that of the projection from TE to area 36 (Saleem et al., 1993b). However, there were a few subtle differences. First, the distribution of terminals in layer I was denser in the TE-to-area 36 projection. Second, the densest distribution within the middle layers tended to be limited to layer IV in most of the projection foci in the TEO-to-TE projection, whereas the densest distribution covered layer III to the upper part of layer V in the TE-to-area 36 projection. Many of the cortico-cortical connections in the prefrontal cortex (Goldman and Nauta, 1977; Bugbee and Goldman-Rakic, 1983; Goldman-Rakic, 1984; Selemon and Goldman-Rakic, 1988; McGuire et al., 1991; Stanton et al., 1993) and the parietal cortex (Cavada and Goldman-Rakic, 1989a,b; Andersen et al., 1990; Blatt et al., 1990) showed a laminar distribution of terminals similar to that in the TE-to-area 36 projection. It may be suggested that the specific termination in layer IV becomes less prominent, whereas the termination in layer I becomes more prominent as the connection extends farther away from the primary sensory areas.

Webster et al. (1991) reported that the projection from TEad to the perirhinal cortex terminated in all layers in infant monkeys, whereas it was confined to layer IV in adult monkeys. The pattern we observed seems to be more similar to their infant pattern than to their adult pattern. The possibility that our subjects were not as old as theirs can be excluded because the range of body weight of our monkeys was similar to that of their adult monkeys and because the projection pattern to the amygdaloid complex in our monkeys was similar to that observed in their adult monkeys (K. Cheng, K.S. Saleem, and K. Tanaka, unpublished observations). The difference in the tracer, and probably a difference in emphasis, may explain the apparently different conclusion.

The reconstruction of single axons confirmed our conclusion that the projection is not limited to layer IV. Most of the reconstructed axons projecting from TE to area 36 had arbors of elongated shape, which expanded from layer VI, V, or IV to layer I or II. We did not find axons with arbors limited to layer IV. This

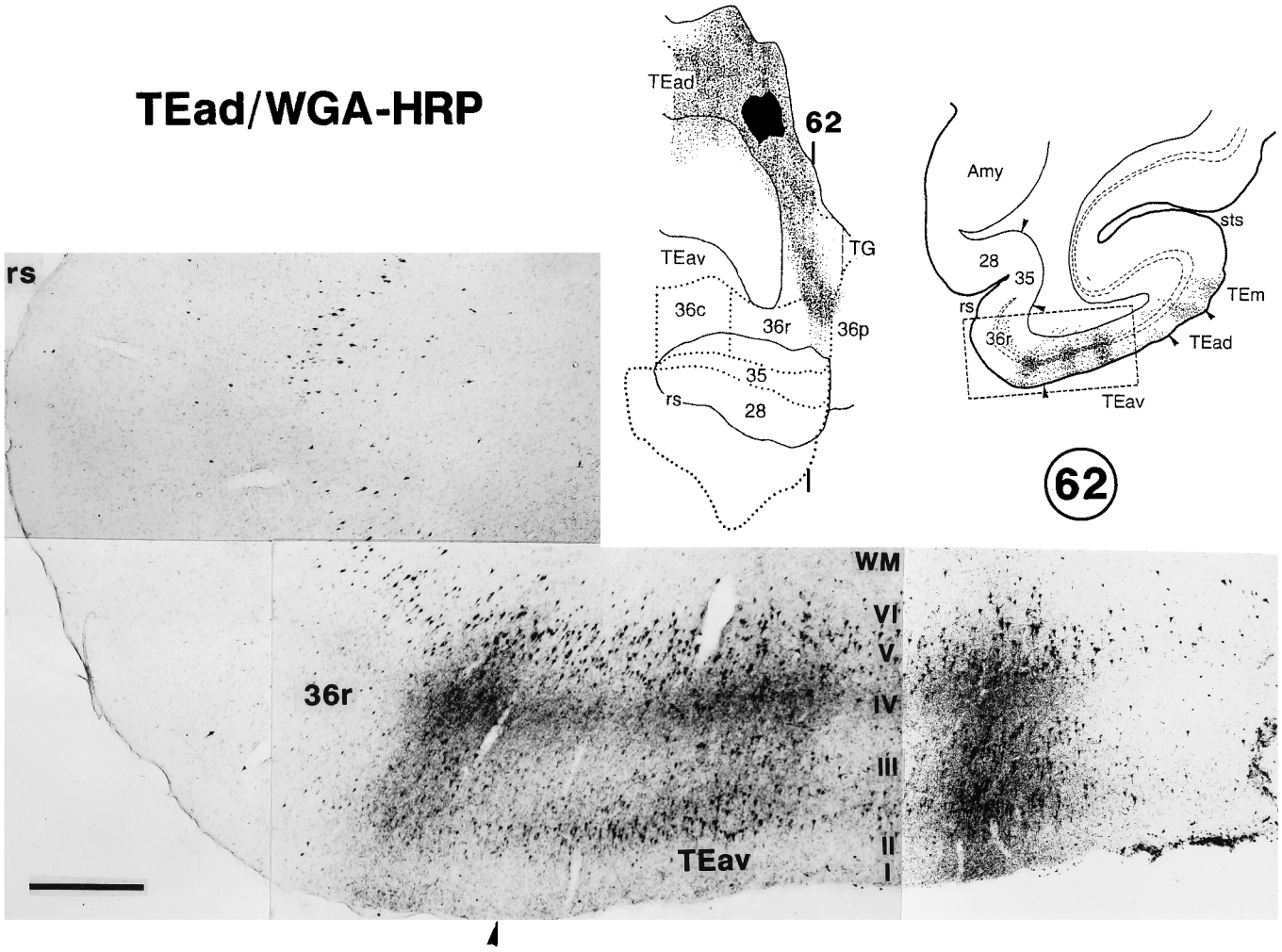

Figure 17. Photomicrograph illustrating the retrogradely labeled neurons and anterogradely labeled terminals in TEav and area 36r, after WGA-HRP injection into TEad. This photomicrograph was taken from the circumscribed area of section *62* illustrated at the *top right*. Its caudorostral level is indicated by the *thin line* in the *top middle* drawing, which is the same as Figure 8*D*. The distribution of labeled neurons extended more medially, beyond the medial limit of the distribution of labeled terminals. Scale bar, 0.5 mm.

contrasts with the TEO-to-TE projections, in which nearly equal numbers of axons showed arbors limited to in and around layer IV, ones limited to the upper layers, and columnar ones (Saleem et al., 1993b). Although only one axon was reconstructed that had arbors limited to the superficial layers in the TE-to-area 36 projection, we believe that the proportion is an underestimate, because the labeled terminals in layers I and II often were too thin to follow over many sections.

We have found that projections from both TEav and TEad had core regions in area 36 of the perirhinal cortex. They were elongated in the caudorostral direction. The caudorostral elongation of the core regions was also observed in the TEO-to-TE projection (Saleem et al., 1993b), but the elongation was more prominent in the TE-to-area 36 projection. The caudorostral elongation was also observed in the intrinsic connections within TEav and TEad (see Figs. 7, 8). These findings suggest that structures are in general aligned in the caudorostral directions in these cortical regions. The caudorostral elongation was also found in the cortico-cortical connections in the frontal cortex (Selemon and Goldman-Rakic, 1988) and the parietal cortex (Andersen et al., 1990), and in cortico-subcortical connections of the frontal cortex (Jakab et al., 1994).

Backward projection

The reciprocality of connections between cortical areas has been emphasized frequently, but evidence has been accumulated that the backward projection is more distributed than the forward projection. Krubitzer and Kaas (1989) and Shipp and Zeki (1989a,b) have found that the backward projection from MT covers different compartments in V1 and V2, whereas the forward projection to MT originates in particular compartments in V1 and V2. Rockland and her colleagues, including the present authors (Douglas and Rockland, 1992; Rockland and Van Hoesen, 1994; Rockland et al., 1994), and Bullier and colleagues (Kennedy and Bullier, 1985; Perkel et al., 1986) have found that the backward projection along the ventral visual cortical pathway reached early stages with steps more than the limit of forward connections. For example, area TEO projected back to V1 and area TE projected to V2 and V1, whereas there were no forward projections in these combinations. The present study showed that this is also true for the connections of TE with the perirhinal cortex and the entorhinal cortex, that is, the distribution of cells-of-origin of the backward projections was wider than that of terminals in the case of forward projection.

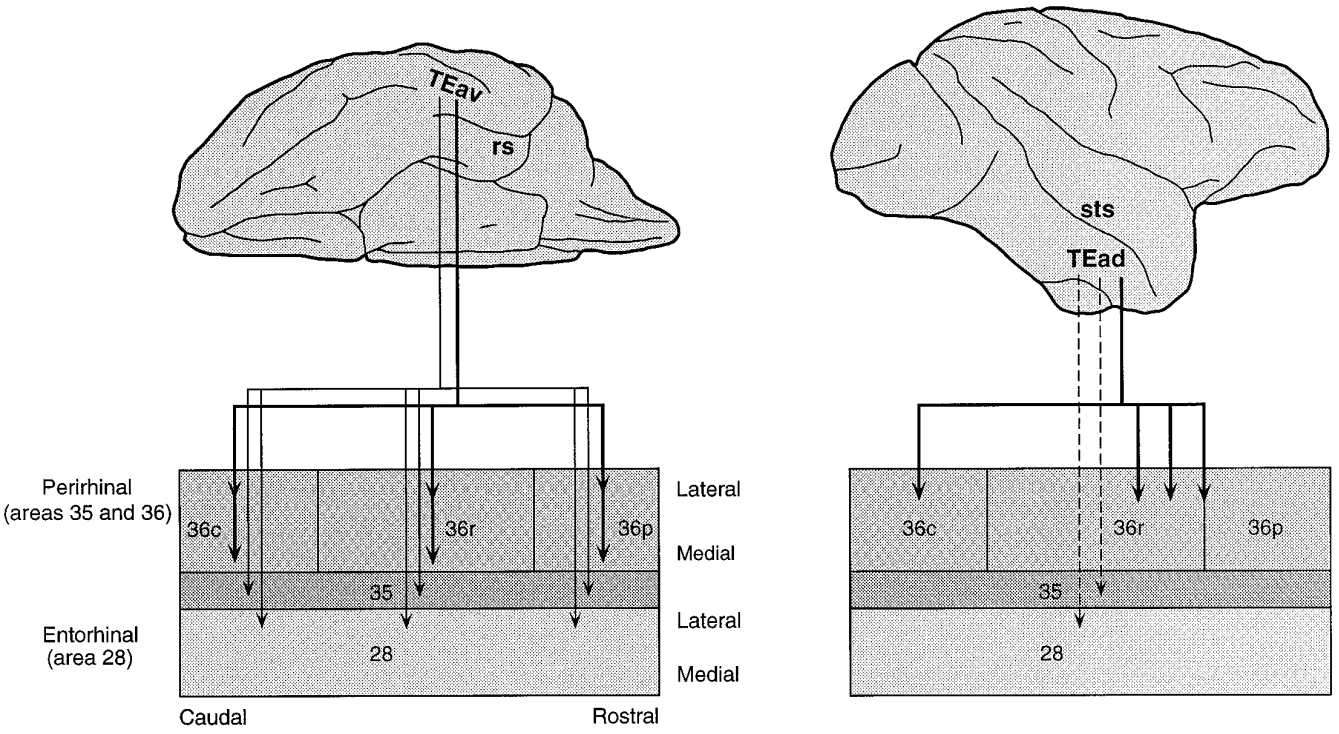

Figure 18. Summary diagram of the projections from TEav (*left*) and TEad (*right*) to the perirhinal and entorhinal cortices. *Heavy solid lines* indicate dense projection, *thin solid lines* denote moderate projection, and *broken lines* indicate weak projection.

REFERENCES

Amaral DG, Insausti R, Cowan WM (1987) The entorhinal cortex of the monkey. I. Cytoarchitectonic organization. J Comp Neurol 264:326–355.

Andersen RA, Asanuma C, Essick G, Siegel RM (1990) Corticocortical connections of anatomically and physiologically defined subdivisions within the inferior parietal lobule. J Comp Neurol 296:65–113.

Blatt GJ, Andersen RA, Stoner GR (1990) Visual receptive field organization and cortico-cortical connections of the lateral intraparietal area (area LIP) in the macaque. J Comp Neurol 299:421–445.

Boussaoud D, Desimone R, Ungerleider LG (1991) Visual topography of area TEO in the macaque. J Comp Neurol 306:554–575.

Brodmann K (1905) Beitrage zur histologisichen Lokalisation der Grosshirnrinde. III. Mitteilung: die rindenfelder der niederen affen. J Psych Neurol 4:177–226.

Bugbee NM, Goldman-Rakic PS (1983) Columnar organization of corticocortical projections in squirrel and rhesus monkeys: similarity of column width in species differing in cortical volume. J Comp Neurol 220:355–364.

Cavada C, Goldman-Rakic PS (1989a) Posterior parietal cortex in rhesus monkey. I. Parcellation of areas based on distinctive limbic and sensory corticocortical connections. J Comp Neurol 287:393–421.

Cavada C, Goldman-Rakic PS (1989b) Posterior parietal cortex in rhesus monkey. II. Evidence for segregated corticocortical networks linking sensory and limbic areas with the frontal lobe. J Comp Neurol 287:422–445.

Dean P (1976) Effects of inferotemporal lesions on the behavior of monkeys. Psychol Bull 83:41–71.

Desimone R, Fleming J, Gross CG (1980) Prestriate afferents to inferior temporal cortex: an HRP study. Brain Res 184:41–55.

DeYoe EA, Felleman DJ, Van Essen DC, McClendon E (1994) Multiple processing streams in occipitotemporal visual cortex. Nature 371:151–154.

Douglas KL, Rockland KS (1992) Extensive visual feedback connections from ventral inferotemporal cortex. Soc Neurosci Abstr 18:390.

Eacott MJ, Gaffan D, Murray EA (1994) Preserved recognition memory for small sets, and impaired stimulus identification for large sets, following rhinal cortex ablations in monkeys. Eur J Neurosci 6:1466–1478.

Felleman DJ, Van Essen DC (1991) Distributed hierarchical processing in the primate cerebral cortex. Cereb Cortex 1:1–47.

Fujita I, Tanaka K, Ito M, Cheng K (1992) Columns of visual features of objects in monkey inferotemporal cortex. Nature 360:343–346.

Gaffan D (1994) Dissociated effects of perirhinal cortex ablation, fornix transection and amygdalectomy: evidence for multiple memory systems in the primate temporal lobe. Exp Brain Res 99:411–422.

Gaffan D, Murray EA (1992) Monkeys (*Macaca fascicularis*) with rhinal cortex ablations succeed in object discrimination learning despite 24 hr intertrial intervals and fail at matching to sample despite double sample presentations. Behav Neurosci 106:30–38.

Gerfen CR, Sawchenko PE (1984) An anterograde neuroanatomical tracing method that shows the detailed morphology of neurons, their axons and terminals: immunohistochemical localization of an axonally transported plant *Phaseolus vulgaris* leucoagglutinin (PHA-L). Brain Res 290:219–238.

Gibson AR, Hansma DI, Houk JC, Robinson FR (1984) A sensitive low artifact TMB procedure for the demonstration of WGA-HRP in the CNS. Brain Res 298:235–241.

Goldman-Rakic PS (1984) Modular organization of prefrontal cortex. Trends Neurosci 7:419–424.

Goldman PS, Nauta WJH (1977) Columnar distribution of corticocortical fibers in the frontal association, limbic, and motor cortex of the developing rhesus monkey. Brain Res 122:393–413.

Gross CG (1973) Visual functions of inferotemporal cortex. In: Handbook of sensory physiology, Vol VIII, Part 3B (Jung R, ed), pp 451–482. Berlin: Springer.

Higuchi S, Miyashita Y (1996) Formation of mnemonic neuronal responses to visual paired associates in inferotemporal cortex is impaired by perirhinal and entorhinal lesions. Proc Natl Acad Sci USA 93:739–743.

Horel JA (1996) Perception, learning and identification studied with reversible suppression of cortical visual areas in monkeys. Behav Brain Res, in press.

Horel JA, Pytko DE (1982) Behavioral effect of local cooling in temporal lobe of monkeys. J Neurophysiol 47:11–22.

Horel JA, Pytko-Joiner DE, Voytko ML, Salsbury K (1987) The performance of visual tasks while segments of the inferotemporal cortex are suppressed by cold. Behav Brain Res 23:29–42.

Insausti R, Amaral DG, Cowan WM (1987) The entorhinal cortex of the monkey. II. Cortical afferents. J Comp Neurol 264:356–395.

Ito M, Fujita I, Tamura H, Tanaka K (1994) Processing of contrast polarity of visual images in the inferotemporal cortex of the macaque monkey. Cereb Cortex 5:499–508.

Ito M, Tamura H, Fujita I, Tanaka K (1995) Size and position invariance of neuronal responses in monkey inferotemporal cortex. J Neurophysiol 73:218–226.

Iwai E, Yukie M (1987) Amygdalofugal and amygdalopetal connections with modality-specific visual cortical areas in macaques (*Macaca fuscata, M. mulatta*, and *M. fascicularis*). J Comp Neurol 261:362–387.

Iwai E, Yukie M (1988) A direct projection from hippocampal field CA1 to ventral area TE of inferotemporal cortex in the monkey. Brain Res 444:397–401.

Iwai E, Yukie M, Suyama H, Shirakawa S (1987) Amygdalar connections with middle and inferior temporal gyri of the monkey. Neurosci Lett 83:25–29.

Jakab RL, Howard R, Goldman-Rakic PS (1994) Small PHA-L injections in prefrontal areas label longitudinal striatal domains in the rhesus monkey. Soc Neurosci Abstr 20:333.

Kennedy H, Bullier J (1985) A double-labelling investigation of the afferent connectivity to cortical areas V1 and V2 of the macaque monkey. J Neurosci 5:2815–2830.

Kobatake E, Tanaka K (1994) Neuronal selectivities to complex object features in the ventral visual pathway of the macaque cerebral cortex. J Neurophysiol 71:856–867.

Kondo H, Hashikawa T, Tanaka K, Jones EG (1994) Neurochemical gradient along the monkey occipito-temporal cortical pathway. NeuroReport 5:613–616.

Krubitzer LA, Kaas JH (1989) Cortical integration of parallel pathways in the visual system of primates. Brain Res 478:161–165.

Lachica EA, Mavity-Hudson JA, Casagrande VA (1991) Morphological details of primate axons and dendrites revealed by extracellular injection of biocytin: an economic and reliable alternative to PHA-L. Brain Res 564:1–11.

Leonard BW, Amaral DG, Squire LR, Zola-Morgan S (1995) Transient memory impairment in monkeys with bilateral lesions of the entorhinal cortex. J Neurosci 15:5637–5659.

Martin-Elkins CL, Horel JA (1992) Cortical afferents to behaviorally defined regions of the inferior temporal and parahippocampal gyri as demonstrated by WGA-HRP. J Comp Neurol 321:177–192.

Maunsell JHR, Van Essen DC (1983) The connections of the middle temporal visual area (MT) and their relationship to a cortical hierarchy in the macaque monkeys. J Neurosci 3:2563–2586.

McGuire PK, Bates JF, Goldman-Rakic PS (1991) Interhemispheric integration. I. Symmetry and convergence of the corticocortical connections of the left and the right principal sulcus (PS) and the left and the right supplementary motor area (SMA) in the rhesus monkey. Cereb Cortex 1:390–407.

Meunier M, Bachevalier J, Mishkin M, Murray EA (1993) Effects on visual recognition of combined and separate ablations of the entorhinal and perirhinal cortex in rhesus monkeys. J Neurosci 13:5418–5432.

Morel A, Bullier J (1990) Anatomical segregation of two cortical visual pathways in the macaque monkey. Vis Neurosci 4:555–578.

Murray EA (1992) Medial temporal lobe structures contributing to recognition memory: the amygdaloid complex versus the rhinal cortex. In: The amygdala: neurobiological aspects of emotion, memory, and mental dysfunction (Aggleton JP, ed), pp 453–470. New York: Wiley-Liss.

Murray EA, Gaffan D, Mishkin M (1993) Neural substrates of visual stimulus–stimulus association in rhesus monkeys. J Neurosci 13:4549–4561.

Nakamura H, Gattass R, Desimone R, Ungerleider LG (1993) The modular organization of projections from areas V1 and V2 to areas V4 and TEO in macaques. J Neurosci 13:3681–3691.

Perkel DJ, Bullier J, Kennedy H (1986) Topography of the afferent connectivity of area 17 of the macaque monkey: a double-labelling study. J Comp Neurol 253:374–402.

Rockland KS, Pandya DN (1979) Laminar origins and terminations of cortical connections of the occipital lobe in the rhesus monkey. Brain Res 179:3–20.

Rockland KS, Van Hoesen GW (1994) Direct temporal-occipital feedback connections to striate cortex (V1) in the macaque monkey. Cereb Cortex 4:300–313.

Rockland KS, Saleem KS, Tanaka K (1994) Divergent feedback connections from areas V4 and TEO in the macaque. Vis Neurosci 11:579–600.

Saleem KS, Cheng K, Tanaka K (1993a) Organization of projection from the anterior TE (TEa) to the perirhinal (areas 35/36) and frontal cortices in the macaque monkey: PHA-L study. Soc Neurosci Abstr 19:971.

Saleem KS, Tanaka K, Rockland KS (1993b) Specific and columnar projection from area TEO to TE in the macaque inferotemporal cortex. Cereb Cortex 3:454–464.

Saleem KS, Cheng K, Suzuki W, Tanaka K (1994) Differential projection from ventral and dorsal parts of the anterior TE to perirhinal cortex in the macaque monkey. Neurosci Res [Suppl] 19:S201.

Saleem KS, Cheng K, Suzuki W, Tanaka K (1995) Differential cortical projection of dorsal and ventral sub-regions of the area TE in the macaque inferotemporal cortex. IBRO Abstr 4:284.

Selemon LD, Goldman-Rakic PS (1988) Common cortical and subcortical targets of the dorsolateral prefrontal and posterior parietal cortices in the rhesus monkey: evidence for a distributed neural network subserving spatially guided behavior. J Neurosci 8:4049–4068.

Seltzer B, Pandya DN (1978) Afferent cortical connections and architectonics of the superior temporal sulcus and surrounding cortex in the rhesus monkey. Brain Res 149:1–24.

Shipp S, Zeki S (1989a) The organization of connections between areas V5 and V1 in macaque monkey visual cortex. 1:309–332.

Shipp S, Zeki S (1989b) The organization of connections between areas V5 and V2 in macaque monkey visual cortex. 1:333–354.

Shiwa T (1987) Corticocortical projections to the monkey temporal lobe with particular reference to the visual processing pathways. Arch Ital Biol 125:139–154.

Stanton GB, Bruce CJ, Goldberg ME (1993) Topography of projections to the frontal lobe from the macaque frontal eye fields. J Comp Neurol 330:286–301.

Suzuki WA, Amaral DG (1994a) Topographic organization of the reciprocal connections between the monkey entorhinal cortex and the perirhinal and parahippocampal cortices. J Neurosci 14:1856–1877.

Suzuki WA, Amaral DG (1994b) Perirhinal and parahippocampal cortices of the macaque monkey: cortical afferents. J Comp Neurol 350:497–533.

Suzuki WA, Zola-Morgan S, Squire LR, Amaral DG (1993) Lesions of the perirhinal and parahippocampal cortices in the monkey produce long-lasting memory impairment in the visual and tactual modalities. J Neurosci 13:2430–2451.

Tanaka K (1996) Inferotemporal cortex and object vision. Annu Rev Neurosci 19:109–139.

Tanaka K, Saito H, Fukada Y, Moriya M (1991) Coding visual images of objects in the inferotemporal cortex of the macaque monkey. J Neurophysiol 66:170–189.

Turner BH, Mishkin M, Knapp M (1980) Organization of the amygdalopetal projections from modality-specific cortical association areas in the monkey. J Comp Neurol 191:515–543.

Van Hoesen GW, Pandya DN (1975a) Some connections of the entorhinal (area 28) and perirhinal (area 35) cortices of the rhesus monkey. I. Temporal lobe afferents. Brain Res 95:1–24.

Van Hoesen GW, Pandya DN (1975b) Some connections of the entorhinal (area 28) and perirhinal (area 35) cortices of the rhesus monkey. III. Efferent connections. Brain Res 95:39–59.

von Bonin G, Bailey P (1947) The neocortex of *Macaca mulatta*. Urbana, IL: University of Illinois.

Webster MJ, Ungerleider LG, Bachevalier J (1991) Connections of inferior temporal areas TE and TEO with medial temporal-lobe structures in infant and adult monkeys. J Neurosci 11:1095–1116.

Witter MP, Amaral DG (1991) Entorhinal cortex of the monkey. V. Projections to the dentate gyrus, hippocampus, and subicular complex. J Comp Neurol 307:437–459.

Yukie M, Iwai E (1988) Direct projections from the ventral TE area of the inferotemporal cortex to hippocampal field CA1 in the monkey. Neurosci Lett 88:6–10.

Yukie M, Takeuchi H, Hasegawa Y, Iwai E (1990) Differential connectivity of inferotemporal area TE with the amygdala and the hippocampus in the monkey. In: Vision, memory, and the temporal lobe (Iwai E, Mishkin M, eds), pp 129–135. New York: Elsevier.

Yukie M, Hikosaka K, Iwai E (1992) Organization of cortical visual projections to the dorsal and ventral parts of area TE of the inferotemporal cortex in macaques. Soc Neurosci Abstr 18:294.

Zeki SM, Shipp S (1989) Modular connections between areas V2 and V4 of macaque monkey visual cortex. Eur J Neurosci 1:494–506.

Zola-Morgan S, Squire LR, Amaral DG, Suzuki WA (1989) Lesions of perirhinal and parahippocampal cortex that spare the amygdala and hippocampal formation produce severe memory impairment. J Neurosci 9:4355–4370.